JCTC Journal of Chemical Theory and Computation

Article

pubs.acs.org/JCTC

Interactions between Methane and Polycyclic Aromatic Hydrocarbons: A High Accuracy Benchmark Study

Daniel G. A. Smith and Konrad Patkowski*

Department of Chemistry and Biochemistry, Auburn University, Auburn, Alabama 36849, United States

Supporting Information

ABSTRACT: Minimum energy structures and interaction energies are obtained for a series of polycyclic aromatic hydrocarbons (PAHs) interacting with a methane molecule. The PAHs include benzene, naphthalene, anthracene, phenanthrene, tetracene, pyrene, and coronene. Interaction energies are calculated using the highest level of theory and basis set available, that is, complete-basis-set extrapolated MP2 plus a conventional or explicitly correlated CCSD(T) correction in moderately sized basis sets. The results show that the singly coordinated minimum configuration observed earlier for benzene−methane is no longer the global minimum one for naphthalene and larger PAHs. Instead, triply coordinated geometries are lower in energy. The global minimum structures for methane interacting with extended systems like graphene sheets and carbon nanotubes are likely to be triply coordinated as well. A variety of novel dispersion-including DFT approaches are compared against the wave-function-based benchmark potential energy curves. The top performer, the B3LYP functional combined with the -D3 dispersion correction, is then employed to calculate interaction energies for methane interacting with hexabenzocoronene and circumcoronene in order to estimate the methane adsorption energy on graphite. The delicate balance between dispersion and exchange in PAH−methane interactions is elucidated using symmetry-adapted perturbation theory with a DFT description of monomers. The present study provides an important benchmark for the design and tuning of more approximate methods for an accurate description of hydrocarbon physisorption on carbon nanostructures.

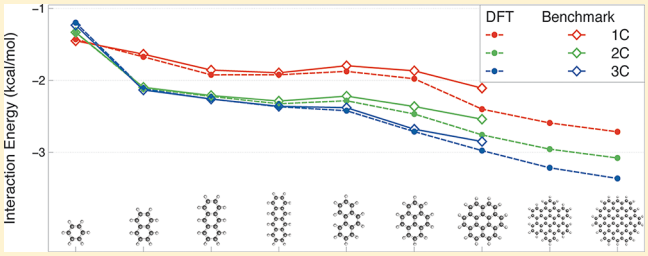

1. INTRODUCTION

Weak intermolecular interactions, especially those dominated by dispersion, are a challenge for *ab initio* quantum chemistry because of a simultaneous need for a nearly complete one-electron basis set and a high-level treatment of electron correlation.[1] Fulfilling the first of these needs is substantially aided by complete-basis-set (CBS) extrapolations,[2,3] bond functions,[4] and, most recently, the explicitly correlated R12 and F12 approaches.[5,6] As far as the second need is concerned, the "gold standard" of electronic structure theory, the single-reference coupled-cluster method with single, double, and noniterative triple excitations [CCSD(T)], provides weak interaction energies accurate to a few percent (with a notable exception of systems where significant static correlation is present[7]) as long as the basis set is sufficiently large. However, the computational cost of a CCSD(T) calculation scales like N^7 with the system size and becomes prohibitively expensive even for moderately large dimers. Therefore, significant effort is being invested in devising methods that produce accurate weak interaction energies and exhibit a more favorable scaling. While density functional theory (DFT) using standard functionals fails remarkably for dispersion-dominated interaction energies,[8,9] many novel DFT approaches are quite successful at accounting for dispersion.[10−21] At the same time, the typical overestimation of dispersion by second-order Møller−Plesset perturbation theory (MP2) is addressed by various spin-component-scaled and related wave-function-based approaches.[22−26] Hybrid wave-function-DFT methods[27−30] also deliver comparable accuracy. The DFT- and MP2-based approaches scale like N^4 or N^5 and can be applied to interactions of much larger systems than CCSD(T). On the other hand, the accuracy of these methods varies, and extensive benchmarking is necessary to determine which of them are appropriate for studying weak interactions at a desired level of accuracy.

The set of high-quality benchmark interaction energies available today is quite impressive. While most older benchmark sets focused on interaction energies near the respective van der Waals minima,[31−33] it was realized, most notably by Sherrill and collaborators, that the accuracy at the minima is not necessarily retained throughout the entire range of intermolecular distances. Therefore, newer benchmark sets include intermolecular distances both smaller and larger than the minimum separations.[34−37] At the same time, the accuracy of some of the older benchmarks, most notably the S22 set,[33] was considerably improved.[38−41] Extensive studies of the performance of various approximate DFT- and MP2-based approaches have been carried out,[42] and while some methods are clearly better than others, there is no single winner that accurately

Received: October 11, 2012
Published: November 7, 2012

   dx.doi.org/10.1021/ct3008809 | J. Chem. Theory Comput. 2013, 9, 370−389

reproduces high-accuracy benchmark interaction energies across the entire spectrum of systems. Therefore, any application of approximate DFT or wave function theories to a class of systems of practical interest should be accompanied by a verification that the chosen approach satisfactorily recovers benchmark interaction energies for similar systems. Such a verification is the heart of the present work, and the goal behind it is a better understanding of hydrocarbon physisorption on graphene sheets[43] and carbon nanotubes.[44]

The adsorption of molecules on carbon nanostructures has been the subject of numerous experimental and theoretical studies.[45] The ability of graphene and nanotubes to effectively bind hydrogen makes these structures a viable medium for hydrogen storage,[46] a critical issue on the road toward clean hydrogen-based energy. The adsorption of methane, and of other small hydrocarbons, on carbon nanostructures is another highly active area of research due to its importance for natural gas storage, transport, fuel-cell combustion, and detection.[47,48] It should be noted that physisorption, the process of binding molecules (adsorbates) to surfaces via van der Waals forces,[49] is inherently harder to model computationally[50] than chemisorption (where the adsorbate−surface bonds are covalent). In particular, an accurate treatment of dispersion energy is absolutely crucial. Nevertheless, the majority of existing computational studies of physisorption use either empirical, Lennard-Jones interaction potentials, or standard density functionals like LDA, B3LYP,[51,52] or PBE.[53] While such approaches can yield useful qualitative results,[54−56] their accuracy is inherently limited. Indeed, studies for model systems indicate that the performance of standard density functionals for carbon-nanostructure adsorption is inferior[57] to that of novel functionals like M05-2X.[13] The use of state-of-the-art accurate N^4 and/or N^5 methods, paired with their careful benchmarking against near-CBS CCSD(T) interaction energies, is required to develop more accurate physisorption potentials. For the hydrocarbon physisorption on carbon nanostructures, the natural choice of model systems for benchmarking is polycyclic aromatic hydrocarbons (PAHs) interacting with methane. The PAHs investigated in this work include benzene, naphthalene, anthracene, tetracene, phenanthrene, pyrene, and coronene.

The benzene−methane complex has been extensively studied using accurate *ab initio* methods (in particular, as a member of the S22[33,39,40] and NBC10[34] test sets). However, CCSD(T)-level interaction energies for complexes of methane with larger PAHs are virtually limited to a single study by Tsuzuki et al.[58] In this reference, lowest-energy structures of the benzene−methane, naphthalene−methane, and pyrene−methane complexes were determined using MP2 calculations in bases up to cc-pVQZ (nonaugmented correlation-consistent quadruple-ζ[59]) plus a CCSD(T) correction in a very small 6-31G* basis. Tsuzuki et al.[58] found that the singly coordinated (1C) structure (with only one of the methane hydrogen atoms closer to the PAH plane than the methane carbon atom) of the benzene−methane global minimum ceases to be the lowest-energy structure for larger PAHs in favor of the doubly coordinated (2C) and triply coordinated (3C) configurations (for which two and three methane hydrogens, respectively, are closer to the PAH plane than the methane carbon). On the basis of the observations of ref 58, it is likely that the benzene−methane complex is an exception rather than the rule, and one needs to go to larger PAHs to even qualitatively recover the adsorption characteristics of extended carbon nanostructures. At the same time, the results of ref 58 are clearly not converged with respect to the basis set, and their accuracy warrants further investigation.

In this work, accurate *ab initio* interaction energies are obtained for the lowest-energy structures of PAH−methane dimers (one lowest-energy structure for each coordination: 1C, 2C, and 3C). We will follow the standard technique employed to generate benchmark interaction energy databases[33] and compute interaction energies as sums of the CBS-extrapolated MP2 contribution and a CCSD(T) correction. The interaction energies obtained in this way for one-dimensional cuts through the potential energy surfaces (passing through the lowest-energy 1C, 2C, and 3C configurations) are then used to gauge the accuracy of a number of modern dispersion-including DFT approaches. Additionally, the relative importance of different interaction energy contributions (electrostatics, induction, dispersion, and exchange) is studied using symmetry-adapted perturbation theory with a DFT description of monomers [SAPT(DFT)].[27,28] The observed trends in the binding energies for different coordinations allow for improved predictions of the adsorption energetics of methane on extended carbon nanostructures. Our approach is somewhat similar in spirit to the hydrogen adsorption study of ref 60 and the water adsorption study of ref 61, where accurate benchmark interaction energies for medium-sized models were used to extrapolate to the case of an infinite graphene sheet. However, our study involves a larger variety of wave-function- and DFT-based approaches all the way through CCSD(T) while refs 60 and 61 employed more approximate DFT/CC and SAPT(DFT) methods, respectively. It should be noted that an extension of our wave function calculations to still larger PAHs, apart from being computationally unfeasible at present, would encounter a serious problem as the increasingly polyradical character of large PAHs[62] inevitably breaks down the single-reference CCSD(T) treatment at some point. Fortunately, such a breakdown does not yet occur for systems studied here, as indicated by reasonably low values of the T1 and D1 coupled-cluster diagnostics.[63]

The structure of the rest of this paper is as follows. In Section 2, the approach used to obtain benchmark interaction energies is specified together with the approximate *ab initio* methods employed and the relevant computational details. The numerical results are presented and discussed in Section 3. Finally, Section 4 presents conclusions.

2. METHODOLOGY AND COMPUTATIONAL DETAILS

The Molpro code[64] was used to obtain all the MP2 and CCSD(T) interaction energies. The MP2 computations utilized density fitting (DF)[65] and employed standard orbital and auxiliary bases aug-cc-pV*X*Z[59,66] and aug-cc-pV*X*Z/MP2FIT,[67,68] respectively. The DF-HF interaction energy and the correlation part of the DF-MP2 interaction energy exhibit mean unsigned errors (MUE; averaged over all benzene−methane and naphthalene−methane complexes at the aug-cc-pVTZ level) of 0.005 and 0.001 kcal/mol, respectively, with respect to the non-density-fitted results. For the points where the comparison is possible at the aug-cc-pVQZ level, the DF-HF error further decreases to 0.001 kcal/mol, and the DF-MP2 error is reduced below convergence thresholds. It is worth noting that the sign and magnitude of the errors remain practically constant across the entire potential curve. As the computational cost of DF-MP2 is a small fraction of that of conventional MP2, only DF-MP2 calculations are feasible in

dx.doi.org/10.1021/ct3008809 | J. Chem. Theory Comput. 2013, 9, 370−389

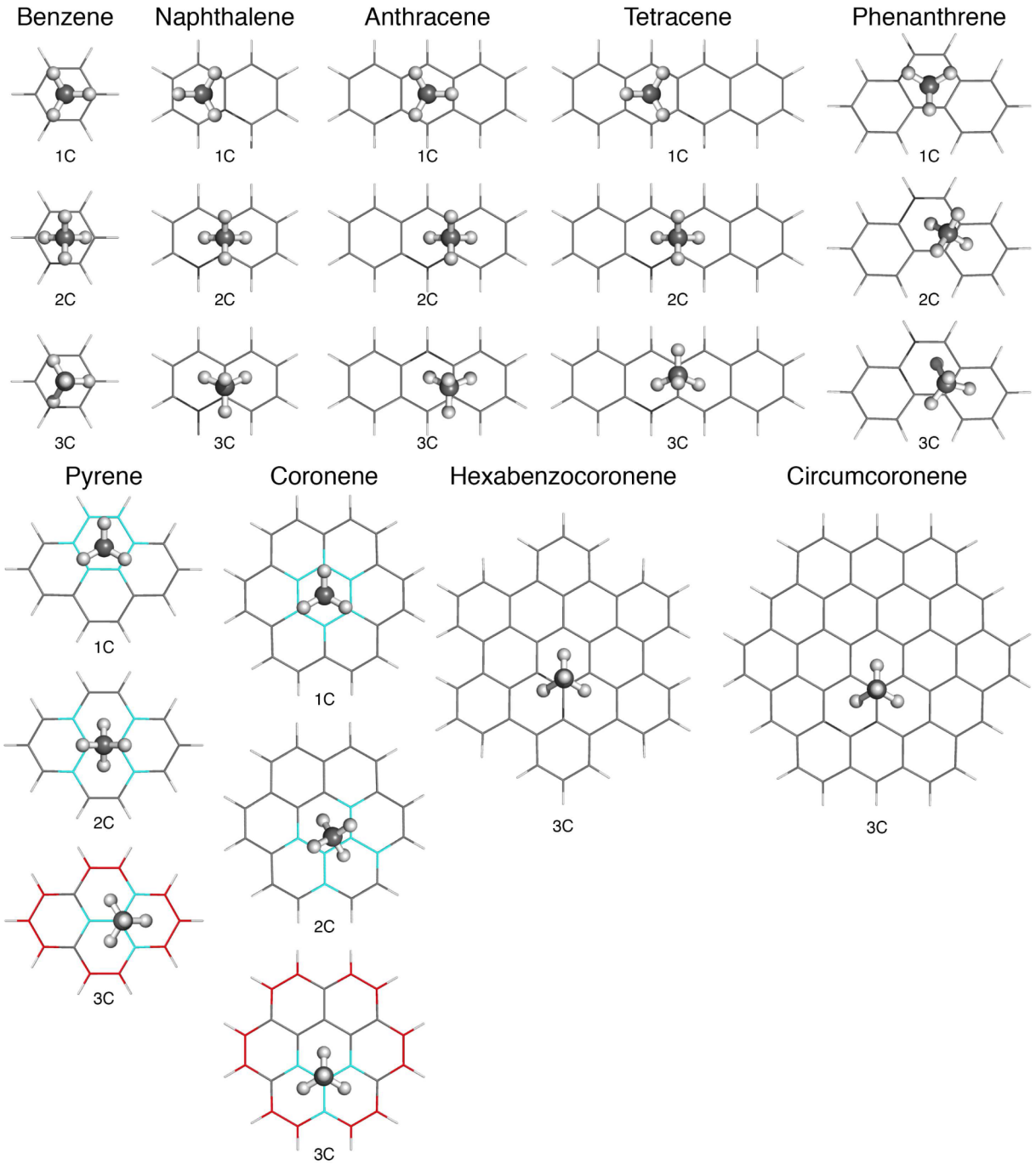

Figure 1. The optimized 1C, 2C, and 3C structures for all dimers considered in the present work. The colors on the pyrene and coronene structures mark carbon atoms that are assigned differently augmented basis sets within the core-DZ and local-DZ approaches—see section 3.1 for details.

quadruple- and quintuple-zeta bases. The "DF-" qualifier will be dropped from now on. The CCSD(T) calculations were performed in the conventional, non-density-fitted way and utilized the aug-cc-pV*X*Z bases. For basis sets involving midbond functions, the additional functions were located halfway between the carbon atom of the methane molecule and the plane of the PAH. These functions were chosen as the hydrogenic set from the same aug-cc-pV*X*Z orbital basis as the atom-centered functions. Unless otherwise stated, all calculations employed the counterpoise (CP) correction for basis set superposition error.[69,70] The 1s carbon electrons were not correlated.

2.1. Geometry Optimizations. To obtain the lowest-energy configurations for each coordination, a three-dimensional scan of the potential energy surface (PES) for a given orientation of methane was first completed at the MP2/aug-cc-pVDZ level, and the most favorable location of methane was narrowed down to 0.01 Å. Full counterpoise-corrected six-dimensional geometry optimizations (that is, only the intramolecular degrees of freedom were frozen) were then run at the MP2/aug-cc-pVTZ level to find the final geometries. The lowest-energy configurations for all three coordinations represent some local minima on the full six-dimensional PES except for 1C phenanthrene—methane and 1C tetracene—methane. The most relevant one-dimensional cuts through the

dx.doi.org/10.1021/ct3008809 | J. Chem. Theory Comput. 2013, 9, 370−389

PES, along the direction z perpendicular to the PAH plane, are then examined. The values of z given throughout the rest of the text are the distances between the methane carbon and the PAH plane. The lowest-energy geometries for each dimer and each coordination are displayed in Figure 1.

2.2. Benchmark Energies from Wave Function Methods. Following the standard practice in the field,[33] the benchmark interaction energy is calculated as

$$E_{\mathrm{int}}^{\mathrm{benchmark}} = E_{\mathrm{int}}^{\mathrm{MP2}}(\text{aug-cc-pV}(X-1)\mathrm{Z},\ \text{aug-cc-pV}X\mathrm{Z}) + \Delta E_{\mathrm{int}}^{\mathrm{CCSD(T)}}(\text{aug-cc-pV}(X'-1)\mathrm{Z},\ \text{aug-cc-pV}X'\mathrm{Z}) \quad (1)$$

where $E_{\mathrm{int}}^{\mathrm{X}} = E_{\mathrm{AB}}^{\mathrm{X}} - E_{\mathrm{A}}^{\mathrm{X}} - E_{\mathrm{B}}^{\mathrm{X}}$ is the supermolecular interaction energy at a given level of theory, $\Delta E_{\mathrm{int}}^{\mathrm{CCSD(T)}} = E_{\mathrm{int}}^{\mathrm{CCSD(T)}} - E_{\mathrm{int}}^{\mathrm{MP2}}$ is the CCSD(T) contribution missing at the MP2 level, and the notation (basis1,basis2) means that the bases "basis1" and "basis2" have been employed in the standard X^{-3} extrapolation for the correlation part of the interaction energy.[2] The SCF part of the interaction energy was taken from the calculation using the larger of the two bases and not extrapolated. We will employ the short-hand notation MP2/(X − 1,X) and ΔCCSD(T)/(X − 1,X) for $E_{\mathrm{int}}^{\mathrm{MP2}}$ (aug-cc-pV(X − 1)Z,aug-cc-pVXZ) and $\Delta E_{\mathrm{int}}^{\mathrm{CCSD(T)}}$ (aug-cc-pV(X − 1)Z,aug-cc-pVXZ), respectively. Moreover, ΔCCSD(T)/aXZ will denote a correction that is computed in the aug-cc-pVXZ≡aXZ basis set and not extrapolated.

To investigate the basis set convergence of the ΔCCSD(T) contribution, explicitly correlated CCSD(T)-F12 calculations were performed for benzene−methane and naphthalene−methane using the Molpro[64] code. The CCSD(T)-F12a and CCSD(T)-F12b approximations[71,72] employ the default explicitly correlated *Ansätze*, geminal parameters, and auxiliary bases. Because the triples contributions to CCSD(T)-F12a and CCSD(T)-F12b do not include explicit correlation (an explicitly correlated (T) correction has been derived only recently[73] and exhibits a steeper computational scaling), we tested the popular estimate of the missing F12 contributions to $\Delta E^{(\mathrm{T})} = E^{\mathrm{CCSD(T)}} - E^{\mathrm{CCSD}}$ via scaling:

$$\Delta E^{(\mathrm{T})-\mathrm{F12}} \approx \Delta E^{(\mathrm{T})} \cdot \frac{E_{\mathrm{corr}}^{\mathrm{MP2}-\mathrm{F12}}}{E_{\mathrm{corr}}^{\mathrm{MP2}}} \quad (2)$$

where the subscript "corr" denotes the correlation energy at a given level of theory. To ensure size consistency, the scaling factor determined for the dimer was also used in the counterpoise-corrected calculations for monomers.[38] The CCSD(T)-F12 approach in its various approximate variants provides greatly improved weak interaction energies in double- and triple-ζ basis sets compared to conventional CCSD(T)[38,74,75] (however, the improvement is somewhat diminished in larger basis sets[76,77]). For the popular S22 database[33] that includes the benzene−methane complex, the MUE of the scaled-triples CCSD(T)-F12b/aDZ method amounts to 0.10 kcal/mol, about a 4-fold improvement over conventional CCSD(T).[75,78]

2.3. DFT Calculations. Out of the many novel variants of DFT proposed to overcome the failure to recover dispersion, the two main groups are the DFT+D approaches (where a more or less empirical dispersion correction is added on top of a standard density-functional calculation) and the functionals specifically optimized for benchmark weak interaction energies. In this work, we tested a few representative members of each group. For DFT+D, we employed the widely popular B3LYP[51,52] and PBE[53] functionals as well as Grimme's reparameterization[12] of Becke's B97 functional.[79] These three functionals were augmented by Grimme's empirical dispersion terms in the -D2[12] and -D3[19] variants. The -D2 and -D3 corrections were calculated using Grimme's DFT+D program V2.1 Rev 6.

The DFT+D interaction energies were calculated using Molpro 2010.1[64] locally modified to include Grimme's reparameterization of B97. The requested energy convergence threshold was 10^{-7} hartree, and the corresponding autogenerated Molpro grids were used. The calculations employed density fitting with the standard cc-pVXZ/JKFIT auxiliary basis sets.[80] It should be noted that the version of B3LYP used was equivalent to the B3LYP card in Gaussian[81] so that the correlation functional contained a VWN3 contribution, not VWN5.[82] As the CP correction is by no means guaranteed to improve DFT results even for dispersion-bound systems, all DFT variants were tested both with and without it.

The second group, the interaction-optimized functionals, included M05-2X,[13] M06-2X,[16] and ωB97X-D.[15] All interaction energies for these functionals were calculated by Gaussian 09[81] using the UltraFine grid that corresponds to a pruned set of 99 radial shells and 590 angular points per atom. While the size of the grid is fairly large, the M05-2X and M06-2X meta-GGA functionals still exhibit small "wiggles" in the interaction potential, especially at medium distances. This effect, which has been noted before for functionals of this kind,[83] could be avoided at still larger grid sizes; however, this would not change any of our conclusions regarding the selection of the best functional(s).

2.4. SAPT(DFT) Analysis. The density-fitted SAPT(DFT) approach[27] (also termed DFT-SAPT[28]) was used to examine the importance of different contributions to the interaction energy. The monomer DFT calculations employed the PBE0 functional[53,84] and were performed using the Dalton code.[85] The developers' version of the SAPT2008 code[86] was used for the subsequent computation of SAPT(DFT) corrections. The Fermi−Amaldi−Tozer−Handy asymptotic correction[87] was employed in all SAPT(DFT) computations, with the monomer ionization potentials taken from the NIST Webbook.[88] The coupled Kohn−Sham (CKS) values of the exchange-induction and exchange-dispersion corrections were computed exactly rather than estimated by scaling the uncoupled results. These exchange corrections were included in the SAPT(DFT) estimates of induction and dispersion energy, respectively, as in previous work.[18] This is especially important for the induction correction which is known to exhibit significant quenching by its exchange-induction counterpart.[89,90]

2.5. Statistical Analysis of Approximate Approaches. At the time when benchmark databases of weak interaction energies contained only near-minimum geometries, the natural measures of the accuracy of a given approximate approach were the mean unsigned error (MUE) and mean unsigned relative error (MURE).[91] For benchmarks that encompass different regions of the PES, neither quantity is, however, particularly relevant. As the energies for different intermolecular separations are widely different, the MUE is strongly influenced by the relative abundance of points from different regions (repulsive, near-minimum, and asymptotic) in the test set. Therefore, the MUE values presented here will refer to the minimum intermolecular separations only and will not include any data for other separations (we will use the name "minima MUE").

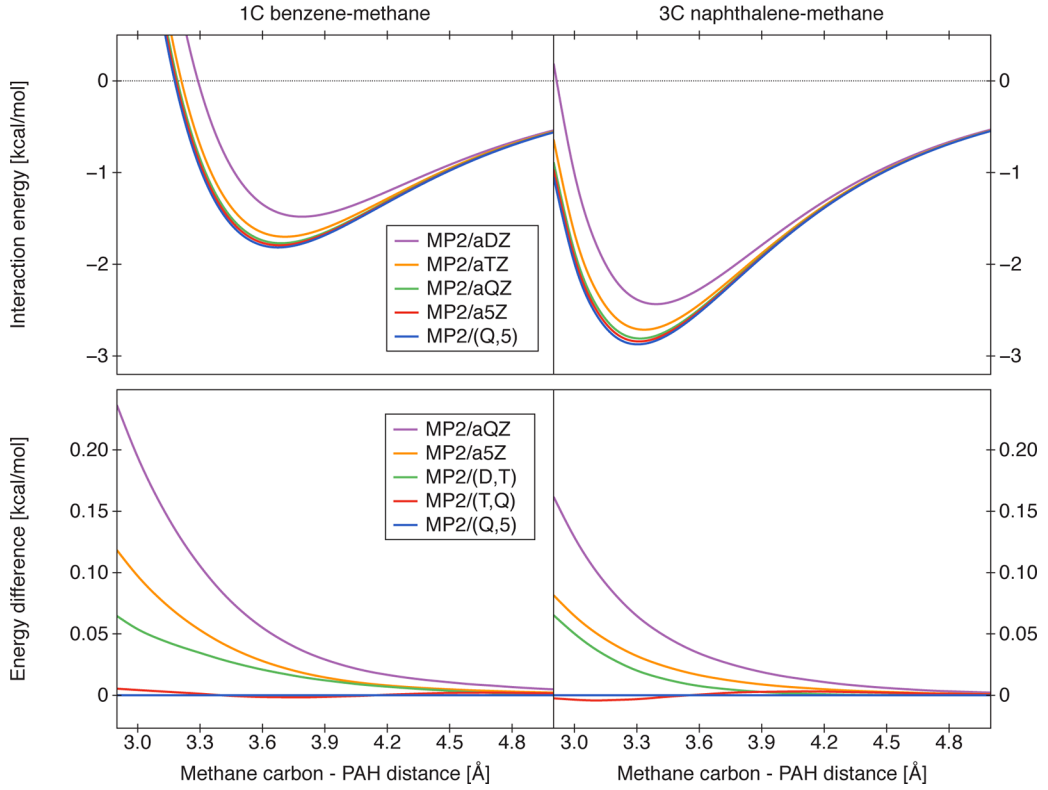

Figure 2. CP-corrected MP2/FC interaction energies (in kcal/mol) for the 1C benzene−methane (left panels) and 3C naphthalene−methane (right panels) complexes as functions of the methane carbon−PAH plane distance z (in Ångstroms). The upper panels display total interaction energies, while the lower panels show interaction energy differences with respect to the highest-level MP2/(Q,5) results.

Table 1. The MP2 and ΔCCSD(T) Contributions to the Benzene−Methane Interaction Energy at the Global-Minimum 1C Configuration with the Methane Carbon−PAH Plane Distance of 3.76 Å[a]

	without midbond				with midbond			
method	D	T	Q	5	D	T	Q	5
MP2	−1.478	−1.691	−1.754	−1.774	−1.551	−1.724	−1.765	−1.780
ext.		−1.777	−1.795	−1.793		−1.794	−1.795	−1.794
MP2-F12	−1.745	−1.785	−1.792	−1.794	−1.760	−1.789	−1.793	−1.794
ext.		−1.802	−1.795	−1.795		−1.803	−1.795	−1.795
ΔCCSD(T)	0.326	0.339	0.349		0.322	0.340	0.352	
ext.		0.345	0.356			0.348	0.360	
ΔCCSD(T)-F12a	0.358	0.358	0.359		0.352	0.356	0.360	
ext.		0.358	0.360			0.358	0.362	
ΔCCSD(T)-F12b	0.343	0.354	0.358		0.330	0.350	0.357	
ext.		0.359	0.361			0.358	0.362	
CCSD(T)/(X−1,X)		−1.438	−1.440			−1.448	−1.435	
MP2/(Q,5)+ΔCCSD(T)/aXZ	−1.468	−1.455	−1.445		−1.472	−1.454	−1.442	
MP2/(Q,5)+ΔCCSD(T)/(X−1,X)		−1.449	−1.437			−1.446	−1.433	
CCSD(T)-F12a/(X−1,X)		−1.449	−1.435			−1.447	−1.434	
MP2-F12/(Q,5)+ΔCCSD(T)-F12a/aXZ	−1.436	−1.436	−1.434		−1.441	−1.437	−1.434	
MP2-F12/(Q,5)+ΔCCSD(T)-F12a/(X−1,X)		−1.436	−1.433			−1.436	−1.432	
CCSD(T)-F12b/(X−1,X)		−1.448	−1.434			−1.447	−1.434	
MP2-F12/(Q,5)+ΔCCSD(T)-F12b/aXZ	−1.450	−1.439	−1.435		−1.463	−1.444	−1.437	
MP2-F12/(Q,5)+ΔCCSD(T)-F12b/(X−1,X)		−1.435	−1.432			−1.436	−1.431	

[a]Conventional and explicitly correlated results in aXZ bases with and without midbond functions (see text for the details of bond functions) are shown as functions of X. The rows marked "ext." display the CBS-extrapolated results where the values in the "X" column were obtained using the (X−1,X) extrapolation. The bottom part of the table contains different estimates of the total CCSD(T)/CBS interaction energy. The (T) triples correction was not scaled in CCSD(T)-F12a but scaled in CCSD(T)-F12b. The energy unit is 1 kcal/mol.

dx.doi.org/10.1021/ct3008809 | J. Chem. Theory Comput. 2013, 9, 370−389

The MURE is, in turn, often dominated by a single data point close to where the interaction energy crosses zero. To avoid this artifactual domination, several modified quantities have been proposed including an energy-dependent weighted average of the relative errors[36] and the *median* unsigned relative error.[92] We will present the latter quantity, averaged over all data points at all intermolecular separations, and denote it as MeURE to stress the difference with respect to the conventional MURE. Additionally, in order to assess the accuracy of the minimum geometries (across a given one-dimensional cut) predicted by different methods, we will use the "minima z difference", the mean absolute deviation of the lowest-energy intermolecular distance z predicted by a given approach from the benchmark value.

3. NUMERICAL RESULTS AND DISCUSSION

3.1. Benchmark Interaction Energies. In this section, we describe how the benchmark wave-function-based PAH–methane interaction energies were obtained using large-basis MP2 and CCSD(T) calculations. The quality of different approximations to the CCSD(T) CBS limit will first be assessed based on the results for the two smallest dimers, benzene–methane and naphthalene–methane. The observations made for these two systems will allow us to select the algorithms to compute benchmark CCSD(T)/CBS interaction energies for larger systems and to estimate their accuracy.

The MP2 interaction energies as functions of the methane carbon–PAH plane distance z are displayed in Figure 2 for 1C benzene–methane (left panels) and 3C naphthalene–methane (right panels). The upper panels in Figure 2 show absolute interaction energies, while the lower panels display differences between various calculated and extrapolated results. The results presented in Figure 2 show that the MP2 interaction energies exhibit smooth convergence with the basis set cardinal number X. This convergence is consistent with the X^{-3} dependence of the correlation energy. As a result, CBS extrapolation improves the results substantially. The smallest-basis extrapolated values, MP2/(D,T), are consistently more accurate than the largest-basis nonextrapolated ones, MP2/a5Z, and the MP2/(T,Q) results are virtually identical to MP2/(Q,5). Thus, basis sets as small as aTZ can be used in the MP2 component as long as the CBS extrapolation is performed.

It is obviously not possible to achieve the same level of basis set saturation in the CCSD(T) approach. Therefore, to understand the effect of basis set size, we first focused on the 1C global minimum of the benzene–methane dimer and obtained an extended set of CCSD(T) interaction energies including results in basis sets up to aQZ, results in bases containing midbond functions, and approximate CCSD(T)-F12 energies. The MP2 and ΔCCSD(T) interaction energy contributions obtained in this way have been gathered in Table 1. The same table contains estimates of the total interaction energy obtained by a straightforward CBS extrapolation of the CCSD(T) results or an augmentation of the MP2/CBS value with the ΔCCSD(T) correction that is either computed or CBS-extrapolated. The main purpose of Table 1 is to assess the accuracy to which the CBS limit can be determined when the system size limits the CCSD(T) basis set choice to aTZ (as is the case for naphthalene–methane) or aDZ (for all PAHs larger than naphthalene). We tested the CCSD(T)-F12 approach with and without the scaling of triples, eq 2, and found that the scaling is beneficial for CCSD(T)-F12b but harmful for CCSD(T)-F12a (the latter observation indicates that the CCSD(T)-F12a approach, formally more approximate than CCSD(T)-F12b,[71] strongly benefits from a cancellation of errors between the CCSD part and the triples part[77]). Therefore, only the unscaled-triples CCSD(T)-F12a results and scaled-triples CCSD(T)-F12b results are listed in Table 1. The interaction energies from all four CCSD(T)-F12 variants can be found in Table SI in the Supporting Information.

The nonextrapolated MP2 and MP2-F12 results in Table 1 all converge smoothly to the CBS limit and demonstrate that the addition of F12 helps more than the addition of midbond functions. Nevertheless, the MP2-F12 results with bond functions are the best out of the four variants. The best non-F12 interaction energy, the a5Z+midbond result, is surpassed in accuracy by MP2-F12 at the aTZ level without midbond functions. Since the interaction energies increase smoothly with the basis set size for all sequences, extrapolation greatly improves the results. All (T,Q) and (Q,5) extrapolated values agree to within 0.002 kcal/mol, and we can establish the value −1.794 ± 0.001 kcal/mol as the benchmark MP2 interaction energy. Although the F12 approach greatly improves the computed MP2 values, Table 1 shows that the non-F12 results become just as accurate upon extrapolation. As all of the MP2 benchmarks for larger systems will be obtained from extrapolations at the (T,Q) or (Q,5) levels, no explicitly correlated treatment of the MP2 contribution will be necessary.

The ΔCCSD(T) corrections shown in Table 1 demonstrate a moderately fast convergence with the basis set size. Extrapolation does assist in the convergence of ΔCCSD(T); however, the results extrapolated from different sequences vary somewhat. The CCSD(T)-F12 approaches, especially CCSD-(T)-F12a, exhibit a faster convergence than conventional CCSD(T). The convergence of ΔCCSD(T)-F12 is smooth for all variants, and extrapolation works very well, with all extrapolated values within 0.004 kcal/mol of each other. The results in Table 1 indicate a benchmark ΔCCSD(T) value of 0.361 ± 0.001 kcal/mol (encompassing all (T,Q)-extrapolated results except for the least accurate one, the conventional CCSD(T) value without midbond functions), which corresponds to the total CCSD(T) interaction energy of −1.433 ± 0.002 kcal/mol.

It is not possible to perform CCSD(T)/aQZ calculations for systems larger than benzene–methane. If the CCSD(T)/aTZ calculations are feasible (as is the case for the naphthalene–methane complex), there exist four sensible ways of estimating the benchmark CCSD(T)/CBS limit from either conventional or explicitly correlated calculations: CCSD(T)/(D,T), MP2/(Q,5)+ΔCCSD(T)/(D,T), MP2/(Q,5)+ΔCCSD(T)/aTZ, and MP2/(Q,5)+ΔCCSD(T)/aDZ. As shown in Table 1, for benzene–methane, these four variants lead to absolute errors of 0.005–0.035 kcal/mol compared to the benchmark interaction energy established using (T,Q) extrapolations of the ΔCCSD(T) term. The addition of midbond functions does not lead to an overall error reduction, and such functions will not be used for subsequent dimers. On the other hand, the explicitly correlated approach clearly improves the basis set convergence, and the F12a- and F12b-based results become virtually identical upon extrapolation. As the accuracy of the (unscaled-triples) F12a approach is probably quite accidental, we will focus on the F12b variant. Out of the four CCSD(T)-F12b-based estimates, the most accurate MP2-F12/(Q,5)+ΔCCSD(T)-F12b/(D,T) approach, with an error of just −0.002 kcal/mol, is also preferred on theoretical grounds as it involves the largest basis sets at each level of theory. As

Table 2. The MP2 and ΔCCSD(T) Contributions to the Naphthalene−Methane Interaction Energy at the Minimum Configurations for Each of the Three Coordinations[a]

method	1C configuration				2C configuration				3C configuration			
	D	T	Q	5	D	T	Q	5	D	T	Q	5
MP2	−1.820	−2.022	−2.080	−2.098	−2.372	−2.619	−2.696	−2.721	−2.433	−2.685	−2.765	−2.791
ext.		−2.102	−2.118	−2.117		−2.730	−2.747	−2.746		−2.801	−2.817	−2.816
ΔCCSD(T)	0.462	0.476			0.624	0.642			0.657	0.677		
ext.		0.483				0.650				0.683		
CCSD(T)/(*X*−1,*X*)		−1.624				−2.088				−2.126		
MP2/(Q,5)+ΔCCSD(T)/a*X*Z	−1.655	−1.640			−2.120	−2.102			−2.159	−2.140		
MP2/(Q,5)+ΔCCSD(T)/(*X*−1,*X*)		−1.634				−2.095				−2.132		
MP2/(Q,5)+ΔCCSD(T)-F12a/a*X*Z	−1.622	−1.621			−2.075	−2.078			−2.113	−2.114		
MP2/(Q,5)+ΔCCSD(T)-F12a/(*X*−1,*X*)		−1.621				−2.079				−2.115		
MP2/(Q,5)+ΔCCSD(T)-F12b/a*X*Z	−1.650	−1.631			−2.109	−2.090			−2.147	−2.127		
MP2/(Q,5)+ΔCCSD(T)-F12b/(*X*−1,*X*)		−1.623				−2.082				−2.119		

[a]The methane carbon−PAH plane distances are equal to 3.73, 3.49, and 3.41 Å for the 1C, 2C, and 3C geometries, respectively. Conventional MP2 and ΔCCSD(T) results in the a*X*Z bases are shown as functions of *X*. The rows marked "ext." display the CBS-extrapolated results where the values in the "*X*" column were obtained using the (*X*−1,*X*) extrapolation. The different estimates of the total CCSD(T)/CBS interaction energy are also given for each configuration including the values that utilize the CCSD(T)-F12a (unscaled triples) and CCSD(T)-F12b (scaled triples) calculations. The energy unit is 1 kcal/mol.

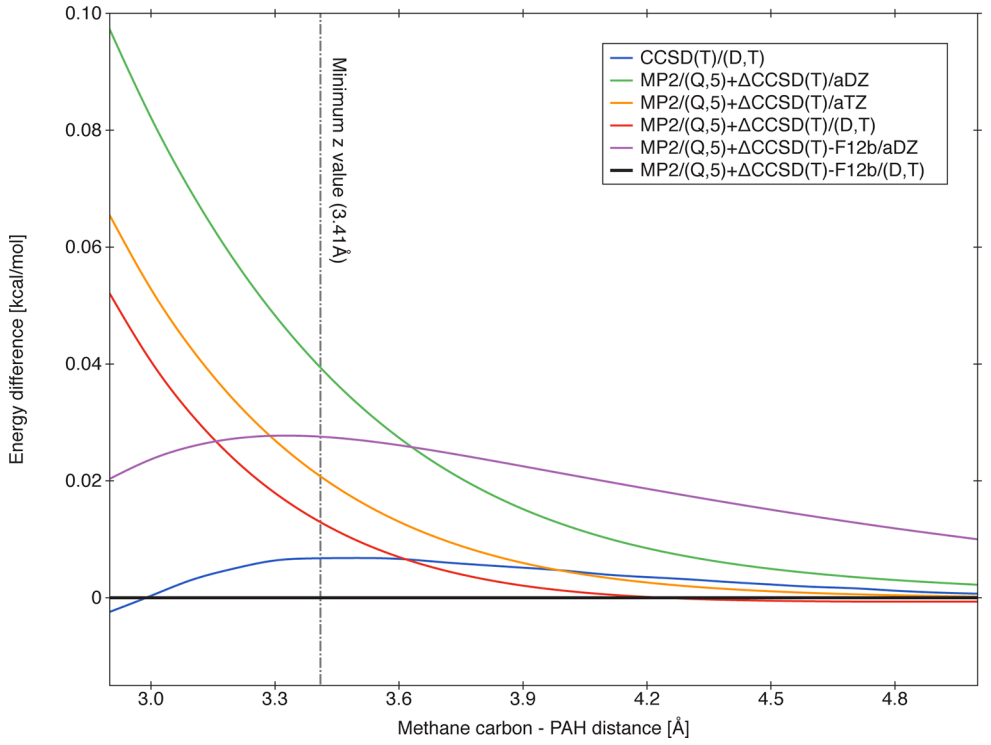

Figure 3. Differences between the benchmark MP2/(Q,5)+ΔCCSD(T)-F12b/(D,T) interaction energy and other CCSD(T)/CBS estimates for the 3C naphthalene−methane complex. The triples term in CCSD(T)-F12b was scaled according to eq 2.

discussed above, the conventional MP2/(Q,5) interaction energy is also virtually converged, and the MP2/(Q,5)+ΔCCSD(T)-F12b/(D,T) approach should be just as accurate but less computationally demanding. We will use the latter theory level to establish the benchmark benzene−methane potential energy curves, as the CCSD(T)/aQZ calculations for more than a few points would be too time-consuming. Overall, the restriction of coupled-cluster calculations to the aTZ basis introduces an error of up to 0.003 kcal/mol (CCSD(T)-F12) or 0.016 kcal/mol (conventional CCSD(T)) in the CCSD(T)/CBS estimate. A further restriction to aDZ increases this error to about 0.02 kcal/mol for CCSD(T)-F12 or 0.04 kcal/mol for conventional CCSD(T). Even this last error, amounting to less than 3% of the interaction energy, is remarkably low, and the results in Table 1 provide strong evidence that our benchmark interaction energies for all systems are highly accurate.

dx.doi.org/10.1021/ct3008809 | J. Chem. Theory Comput. 2013, 9, 370−389

Table 3. The MP2 and ΔCCSD(T) Contributions to Pyrene−Methane and Coronene−Methane Interaction Energies (in kcal/mol) Computed Using Different Partially Augmented Basis Sets Defined in the Text[a]

	pyrene−methane				coronene−methane			
basis	size	1C	2C	3C	size	1C	2C	3C
				MP2				
cc-pVDZ	308	−1.157	−1.484	−1.630	430	−1.493	−1.746	−1.897
local-DZ	369−387	−2.166	−2.741	−3.046	491−509	−2.603	−3.069	−3.362
jun-cc-pVDZ	376	−1.613	−2.073	−2.331	530	−2.057	−2.428	−2.693
core-DZ	427	−2.171	−2.774	−3.141	611	−2.673	−3.133	−3.521
heavy-DZ	461	−2.128	−2.836	−3.028	655	−2.595	−3.051	−3.381
heavy′-DZ	477	−2.221	−2.688	−3.218	671	−2.687	−3.186	−3.559
aug-cc-pVDZ	517	−2.227	−2.853	−3.229	719	−2.691	−3.192	−3.565
CBS		−2.519	−3.198	−3.639		−2.997	−3.543	−3.964
				ΔCCSD(T)				
cc-pVDZ	308	0.581	0.718	0.815	430	0.767	0.868	0.953
local-DZ	369−387	0.656	0.835	0.957	491−509	0.881	1.005	1.115
jun-cc-pVDZ	376	0.614	0.771	0.886	530	0.818	0.948	1.037
core-DZ	427	0.659	0.838	0.963	611	0.894	1.003	1.130
heavy-DZ	461	0.675	0.851	0.974	655			
heavy′-DZ	477	0.660	0.838	0.963	671			
aug-cc-pVDZ	517	0.658	0.836	0.962	719			

[a]A blank space signifies that the CCSD expansion failed to converge due to linear dependencies in the basis set. The MP2/CBS values listed for comparison were obtained from the (Q,5) extrapolation for pyrene−methane and the (T,Q) one for coronene−methane. The size of the local-DZ basis set is slightly different for different coordinations. Thus, a range of values is listed.

The MP2 and ΔCCSD(T) contributions to benchmark naphthalene−methane interaction energies for the deepest minima corresponding to each of the three coordinations (the 3C minimum is the global one) are shown in Table 2 along with the different estimates of the CCSD(T)/CBS limit. As expected, the MP2 interaction energy grows monotonically with basis set size, and all (T,Q) and (Q,5) extrapolations agree to within 0.001 kcal/mol of each other. The conventional ΔCCSD(T) term also exhibits smooth convergence, but the aDZ and aTZ bases are insufficient to narrow this term down to better than 0.01−0.02 kcal/mol. Consequently, the highest-level conventional estimates of the CBS limit, the MP2/(Q,5)+ΔCCSD(T)/(D,T) values, are overestimated by 0.011−0.013 kcal/mol compared to the MP2/(Q,5)+ΔCCSD(T)-F12b/(D,T) result (note how the discrepancies between methods are consistent across all structures). The latter approach, chosen as a benchmark for the benzene−methane potential energy curves based on Table 1, will also be employed to generate benchmark curves for naphthalene−methane. A fair estimate of the accuracy of the benchmark is the difference between the MP2/(Q,5)+ΔCCSD(T)-F12a/(D,T) and MP2/(Q,5)+ΔCCSD(T)-F12b/(D,T) values, which amounts to 0.002−0.004 kcal/mol for the three coordinations. The observed accuracy of the conventional MP2/(Q,5)+ΔCCSD(T)/(D,T) estimates is similar to that found for the benzene−methane dimer. The same is also true for the aDZ-based estimates MP2/(Q,5)+ΔCCSD(T)/aDZ (errors of 0.03−0.04 kcal/mol) and MP2/(Q,5)+ΔCCSD(T)-F12b/aDZ (errors slightly below 0.03 kcal/mol). Thus, the satisfactory accuracy of even the simplest MP2/(Q,5)+ΔCCSD(T)/aDZ estimate is likely transferable to dimers involving larger PAHs. Moreover, unlike the MP2/(Q,5)+ΔCCSD(T)/(D,T) case where the improvement brought about by the F12b approach is enormous, the advantage of MP2/(Q,5)+ΔCCSD(T)-F12b/aDZ over MP2/(Q,5)+ΔCCSD(T)/aDZ is quite modest and does not justify the additional computational effort. Therefore, all benchmarks for anthracene−methane and larger complexes will employ the conventional MP2/(Q,5)+ΔCCSD(T)/aDZ level.

Figure 3 demonstrates the differences between the benchmark MP2/(Q,5)+ΔCCSD(T)-F12b/(D,T) value and various other CCSD(T)/CBS estimates for the 3C naphthalene−methane complex over the relevant range of z distances. At a minimum separation of 3.41 Å, all six extrapolation schemes agree to within 0.04 kcal/mol. Out of the four non-F12 schemes, the CCSD(T)/(D,T) extrapolation performs best at the minimum and at shorter distances. This is quite surprising as, without extrapolation, the CCSD(T)/aTZ curve differs from the benchmark by 0.1−0.3 kcal/mol in this z range, much more than any of the MP2/(Q,5)+ΔCCSD(T) variants. Therefore, the performance of CCSD(T)/(D,T) likely benefits from a fortunate cancellation of errors. The conventional MP2/(Q,5)+ΔCCSD(T) estimates start deviating from the benchmark in the repulsive region, which indicates that the short-range dynamical correlation (interelectronic cusp[5]) effects, which are poorly reproduced by conventional Gaussian basis sets, become increasingly important. For large z, the CCSD(T)/(D,T) approach is nearly as accurate as MP2/(Q,5)+ΔCCSD(T)/(D,T) and MP2/(Q,5)+ΔCCSD(T)/aTZ and clearly more accurate than MP2/(Q,5)+ΔCCSD(T)/aDZ. If only the aDZ basis set is available for the ΔCCSD(T) correction, the MP2/(Q,5)+ΔCCSD(T)-F12b/aDZ approach is superior to MP2/(Q,5)+ΔCCSD(T)/aDZ in the repulsive region but inferior at large z, where the latter, simpler alternative becomes increasingly accurate.

The CCSD(T)/aDZ interaction energies can only be obtained for systems up to the size of pyrene−methane. While recent algorithmic improvements and scalable parallel implementations have significantly extended the range of systems for which CCSD(T) calculations are possible,[93−95] the presence of diffuse basis functions on multiple centers inevitably leads to near linear dependencies in the basis set. It is these dependencies and the associated CCSD convergence problems, not the CPU time and/or resource limitations,

dx.doi.org/10.1021/ct3008809 | J. Chem. Theory Comput. 2013, 9, 370−389

that prevented us from calculating the coronene−methane CCSD(T) interaction energies in the full aDZ basis set. To overcome the linear dependency issues, at least some of the offending basis functions have to be removed. A selective removal of diffuse functions has been proposed before[33,96,97] as a way to decrease the number of basis functions without affecting the results significantly—see ref 98 for a systematic study. One of the most popular approaches is the removal of all diffuse functions on hydrogen and helium atoms while keeping all diffuse functions on heavier atoms. The a*XZ* basis sets trimmed in this way have been called aug′-cc-pV*XZ*,[96] heavy-aug-cc-pV*XZ* (heavy-*XZ*),[99] and jul-cc-pV*XZ*, the first member of the "calendar" basis set family.[100] For the purpose of coronene−methane CCSD(T) calculations, we introduce three additional augmentation schemes that successively eliminate basis functions that will likely have little impact on the interaction energy, that is, the diffuse functions located furthest from the region between the interacting molecules. First, as the diffuse functions on methane hydrogens likely play a much more important role than the diffuse functions on coronene hydrogens, we form the heavy′-aug-cc-pVDZ (heavy′-DZ) basis where only diffuse functions from the PAH hydrogens are removed from the full aDZ set. Further basis functions that likely play a small role in the overall interaction energy are the highest-angular-momentum (*d*) diffuse functions on the outermost carbons: their removal from heavy′-DZ leads to a set that will be denoted as core-aug-cc-pVDZ (core-DZ). Finally, an approach where only the methane atoms and the innermost PAH carbon atoms (those within 2.1 Å of the methane carbon's projection onto the PAH plane) retain diffuse functions is labeled as local-aug-cc-pVDZ (local-DZ). Note that all diffuse functions on methane are present in heavy′-DZ, core-DZ, and local-DZ. Pictorial representations of the different augmentation schemes in the pyrene−methane and coronene−methane complexes are displayed in Figure 1. The red colored carbon atoms have the highest angular momentum diffuse functions removed in the core-DZ basis set (the red colored set is the same for all coordinations and has been marked on the 3C structures only). The cyan colored carbon atoms are those that have diffuse functions in the local-DZ basis.

A comparison of the MP2 interaction energies and ΔCCSD(T) corrections computed using different augmentation schemes of the cc-pVDZ basis is shown in Table 3. This table contains results for pyrene−methane (for which we can compute CCSD(T) in all basis sets including full aDZ) and coronene−methane (for which we were not able to converge the CCSD iterations for the most diffuse bases). The results computed using the jun-cc-pVDZ set,[100] obtained from the jul-cc-pVDZ≡heavy-DZ one via a removal of all diffuse *d* functions on carbon atoms, are listed in Table 3 as well.

The pyrene−methane results in Table 3 demonstrate that diffuse functions are quite important for both the MP2 interaction energy and the ΔCCSD(T) correction and should, whenever possible, be included at the aDZ level in order to obtain accurate results. The key question is which diffuse functions play the least important role in the ΔCCSD(T)/aDZ correction. First, in order to examine the importance of diffuse functions on hydrogens, the heavy′-DZ and heavy-DZ basis sets are compared to the full aDZ. The resulting MUE on the three pyrene−methane complexes are 0.002 and 0.014 kcal/mol, respectively. We note that while the removal of diffuse functions from the methane hydrogens has a fairly small impact on the ΔCCSD(T) correction, these functions do not appear to aggravate the linear dependency issues and can be safely included in any augmentation scheme. On the other hand, the diffuse functions on the PAH hydrogens have a very small contribution to the ΔCCSD(T) correction. Therefore, these basis functions are removed in the subsequent augmentation schemes.

The further reduction of diffuse basis functions leading to the core-DZ and local-DZ sets has little impact on the MP2 interaction energy and the ΔCCSD(T) term. For the latter, the pyrene−methane MUE (with respect to the full aDZ set) amount to 0.001 and 0.003 kcal/mol for core-DZ and local-DZ, respectively. It is of interest that both basis sets capture the aDZ interaction energies better than the heavy-DZ basis despite being smaller and causing fewer CCSD convergence problems. In fact, we were able to compute the coronene−methane CCSD(T) interaction energies in both core-DZ and local-DZ but not in heavy-DZ. The results in Table 3 demonstrate that, for the two dimers presented, the differences between the ΔCCSD(T) terms in two basis sets are roughly an order of magnitude smaller than the differences in the MP2 interaction energy. Moreover, the relative accuracies provided by different augmentation schemes are fairly constant across different coordinations.

The pyrene−methane results in Table 3 suggest that the coronene−methane ΔCCSD(T) corrections computed in the core-DZ and local-DZ bases should be within 0.01 kcal/mol from the full aDZ result. Interestingly, the differences between core-DZ and local-DZ for coronene−methane are larger than for pyrene−methane and (slightly) exceed 0.01 kcal/mol for two of the three coordinations. On the basis of the observed CCSD convergence patterns (we could not converge the core-DZ result as tightly as the other ones) and on the behavior of the results as a function of z (not shown), we believe that the primary reason for the larger differences is residual convergence problems affecting the core-DZ result. Nevertheless, the observed level of agreement between core-DZ and local-DZ provides, together with the pyrene−methane results, a strong justification for using the local-DZ basis for our benchmark coronene−methane CCSD(T) calculations and suggests that the additional errors incurred in this way do not exceed 0.01 kcal/mol. Therefore, the benchmark coronene−methane interaction energies will be obtained at the MP2/(T,Q)+ΔCCSD(T)/local-DZ level. Finally, it is worth noting that the importance of particular diffuse functions depends on the proximity of their centers to the interaction region much more strongly than on the type of the atom. Indeed, the lack of diffuse functions on distant PAH carbon atoms in the local-DZ basis set turns out to be a less severe approximation than the lack of diffuse functions on methane hydrogens in the jun-cc-pVDZ and jul-cc-pVDZ≡heavy-DZ bases. Thus, the "calendar" basis sets are not a particularly good choice of partial augmentation for our systems as the CCSD(T) approach does not converge in jul-cc-pVDZ and leads to fairly inaccurate results in jun-cc-pVDZ.

The accuracy of the benchmark results obtained in this section depends both on the accuracy to which the CCSD(T)/CBS limit was determined and on the magnitude of the effects neglected in the rigid-monomer, frozen-core CCSD(T) approach. As expected, the correction for the core−core and core−valence correlation is very small—it amounts to 0.004 kcal/mol for the 1C benzene−methane minimum geometry at the CCSD(T)/aug-cc-pCVTZ level of theory. The monomer

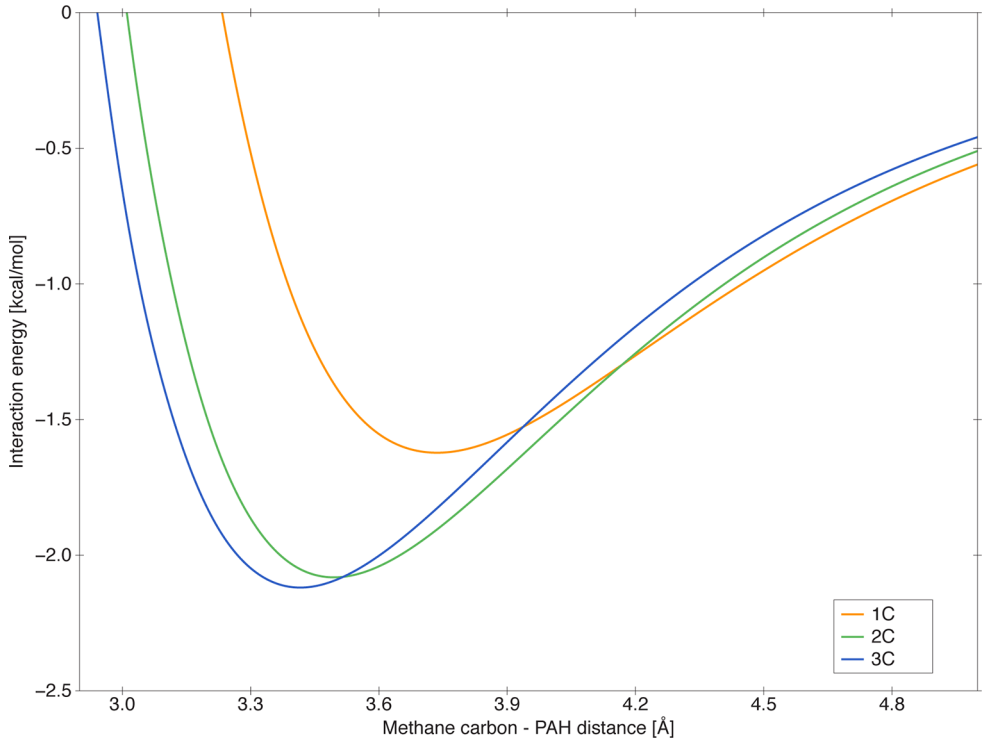

Figure 4. MP2/(Q,5)+ΔCCSD(T)-F12b/(D,T) benchmark interaction potentials for the three coordinations of the naphthalene−methane complex.

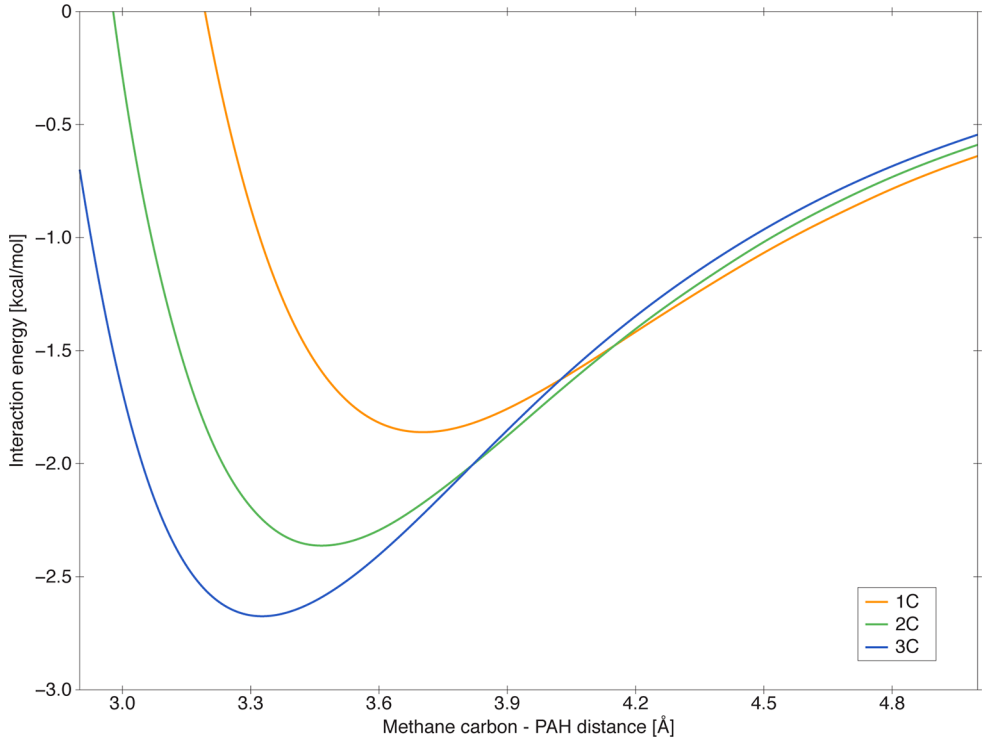

Figure 5. MP2/(Q,5)+ΔCCSD(T)/aDZ benchmark interaction potentials for the three coordinations of the pyrene−methane complex.

flexibility effects can be estimated by comparing the van der Waals well depth obtained with the monomers frozen at their monomer-optimized geometries (as is the case throughout this work) to the well depth computed by minimization of the CP-corrected interaction energy between fully flexible monomers. In the latter case, the specific quantity that needs to be minimized is

$$E_{\text{int}}^{\text{flexible}} = [E^{\text{AB}}(\text{AB}) - E^{\text{AB}}(\text{A}) - E^{\text{AB}}(\text{B})] + [E^{\text{A}}(\text{A}) - E_0^{\text{A}}(\text{A})] + [E^{\text{B}}(\text{B}) - E_0^{\text{B}}(\text{B})] \quad (3)$$

dx.doi.org/10.1021/ct3008809 | J. Chem. Theory Comput. 2013, 9, 370−389

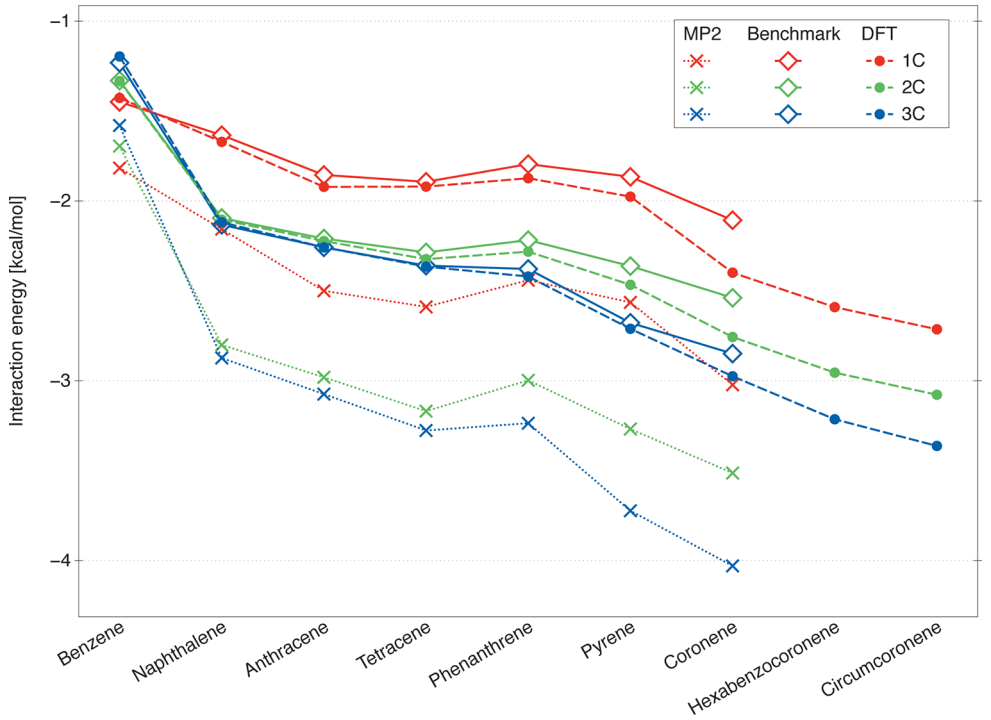

Figure 6. Comparison of the interaction energies calculated by different approaches for the 1C, 2C, and 3C minimum structures (obtained as described in the text) of all PAH−methane dimers considered here. The DFT results are computed at the B3LYP-D3/aDZ level. The MP2 ones are taken from the (Q,5) extrapolation [(T,Q) for coronene], and the "Benchmark" values are calculated at the MP2+ΔCCSD(T) level as described in the text.

where the superscripts denote the basis set (dimer-centered or monomer-centered), the symbols in parentheses denote the subsystems, and the subscript 0 signifies the nonrelaxed optimized geometry of the monomer. For the 1C benzene−methane complex, the flexible well depth obtained by minimizing eq 3 (with the benzene monomer constrained to the D_{6h} symmetry and the dimer to C_{3v} symmetry) at the MP2 level of theory is larger by only 0.005 kcal/mol (aDZ) and 0.001 kcal/mol (aTZ) than the conventional rigid well depth. Moreover, the changes in the bond lengths do not exceed 0.004 Å. To justify the symmetry restriction, we performed a completely unrestricted MP2/aTZ dimer optimization, which lowered the interaction energy further by 0.001 kcal/mol. We conclude that the monomer flexibility effects on the benchmark energies obtained herein do not exceed 0.005 kcal/mol at the minimum.

It is harder to estimate the benchmark uncertainty due to the neglect of coupled-cluster excitations beyond CCSD(T). Such an estimate (although in a very small 6-31G*(0.25) basis set) was obtained for several structures of the benzene dimer by Pitoňák et al.[101] via an approximate account of the quadruple excitations at the CCSD(TQ$_f$) level.[102] The interaction energy contributions beyond CCSD(T) ranged between 0.021 and 0.043 kcal/mol.[101] As the van der Waals well depth for the benzene dimer is about twice as large as for benzene−methane,[33,39,40] the beyond-CCSD(T) effects on the latter quantity are not likely to exceed 0.03 kcal/mol. To verify this, we computed the full CCSDT/6-31G* interaction energy at the 1C benzene−methane minimum using the CFOUR program.[103] The triples effects beyond CCSD(T) decrease the interaction energy by 0.014 kcal/mol. It should be stressed that the 6-31G* basis set, the largest one feasible at this level, is far from adequate—the CCSD(T) interaction energy in this basis is just −0.02 kcal/mol. Nevertheless, the beyond-CCSD(T) effects provide one of the largest contributions to the overall uncertainty of our CCSD(T)/CBS benchmark but should not exceed a few hundredths of a kilocalorie per mole.

Figures 4 and 5 display one-dimensional cuts through the interaction potentials for all three coordinations of the naphthalene−methane and pyrene−methane complexes, respectively. These figures show that the benzene−methane dimer with its 1C global minimum[34,58] is nothing but a special case as the 1C coordination is actually the least binding one for all other PAHs. Moreover, Figures 4 and 5, the analogous graphs for other dimers given in the Supporting Information (Figures S1−S4), and Figure 6, which collects the lowest interaction energies for all systems and all coordinations, illustrate the different character of binding in linear and nonlinear acenes. While the global minima are triply coordinated in all cases, for linear PAHs, the 2C coordination exhibits a local minimum that is only slightly shallower than the 3C one, cf. Figure 6. The nonlinear PAHs clearly favor the 3C configuration—the 2C lowest-energy structures are significantly less binding.

3.2. DFT Calculations. In this section, we examine how well different DFT functionals capture the benchmark interaction energies. At first, we will restrict ourselves to the complexes with the most accurate MP2/(Q,5)+ΔCCSD(T)-F12b/(D,T) benchmark potentials: benzene−methane and naphthalene−methane. On the basis of the performance of different DFT approaches on six one-dimensional potential cuts (the interaction energy as a function of z for 1C, 2C, and 3C orientations of benzene−methane and naphthalene−methane) evaluated using the quantities described in section 2.5, we will determine the best DFT functionals to use for PAH−methane complexes. Subsequently, the best functionals will be compared

dx.doi.org/10.1021/ct3008809 | J. Chem. Theory Comput. 2013, 9, 370−389

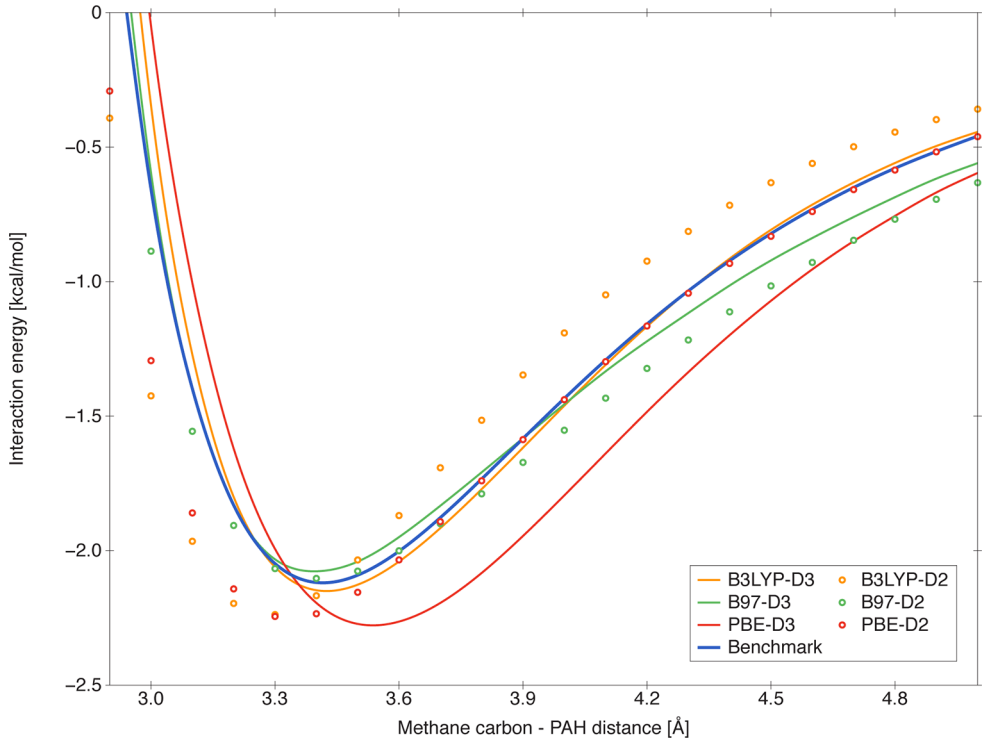

Figure 7. CP-corrected DFT+D/aTZ interaction potentials for the 3C naphthalene−methane complex as compared to the MP2/(Q,5)+ΔCCSD(T)-F12b/(D,T) benchmark.

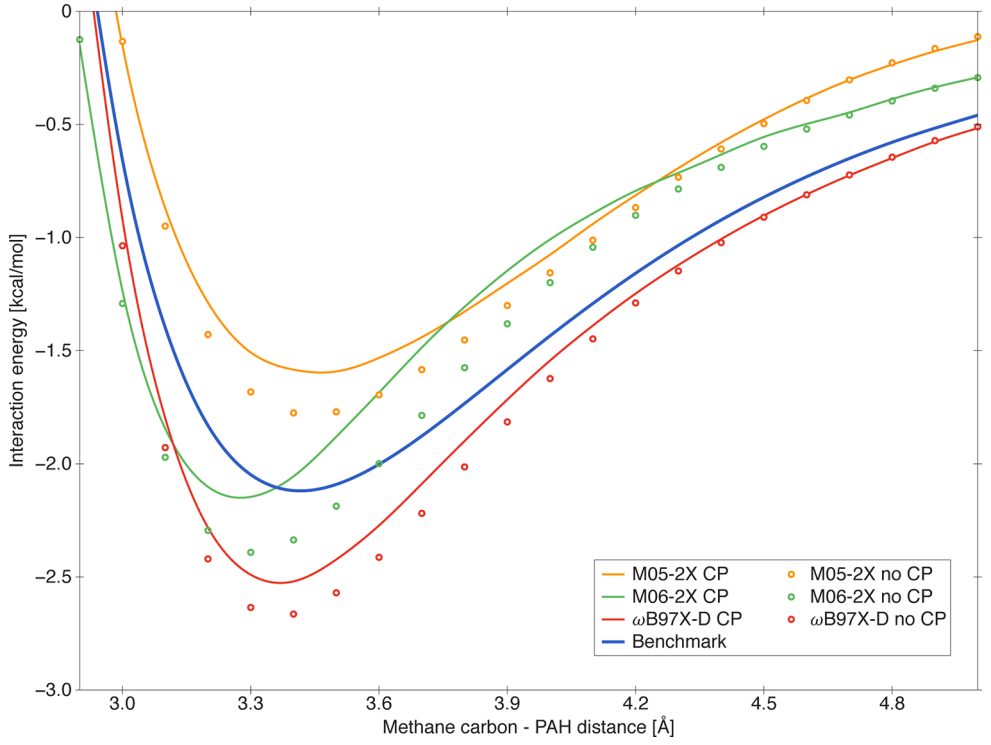

Figure 8. M05-2X, M06-2X, and ωB97X-D interaction potentials computed in the aTZ basis set (with and without the CP correction) for the 3C naphthalene−methane complex as compared to the MP2/(Q,5)+ΔCCSD(T)-F12b/(D,T) benchmark.

against the wave function-based benchmarks for the entire set of complexes to verify whether the good performance on smaller dimers is carried on to larger systems. In the last part, we will employ the best selected DFT variant to larger dimers where no reliable CCSD(T)-level benchmarks can be obtained—the hexabenzocoronene−methane and circumcoronene−methane systems. It should be noted that our DFT results for benzene−methane and naphthalene−methane were calculated using Gaussian[81] without density fitting, while the results for the remaining complexes were obtained with density

dx.doi.org/10.1021/ct3008809 | J. Chem. Theory Comput. 2013, 9, 370−389

Table 4. Minimum Interaction Energies E_{int} and Optimal Methane Carbon−PAH Plane Distances z_{min} Obtained Using Different Density Functionals and aDZ and aTZ Basis Sets for the 1C, 2C, and 3C Structures of Naphthalene−Methane[a]

		1C configuration		2C configuration		3C configuration	
method	basis	z_{min}	E_{int}	z_{min}	E_{int}	z_{min}	E_{int}
benchmark		3.73	−1.623	3.49	−2.082	3.41	−2.119
			CP-corrected				
B3LYP-D2	aDZ	3.60	−1.732	3.34	−2.219	3.27	−2.229
	aTZ	3.59	−1.796	3.34	−2.240	3.28	−2.241
B3LYP-D3	aDZ	3.73	−1.672	3.48	−2.102	3.41	−2.118
	aTZ	3.72	−1.722	3.48	−2.133	3.42	−2.150
B97-D2	aDZ	3.68	−1.710	3.44	−2.103	3.37	−2.127
	aTZ	3.66	−1.754	3.46	−2.091	3.40	−2.103
B97-D3	aDZ	3.72	−1.685	3.44	−2.106	3.37	−2.101
	aTZ	3.70	−1.726	3.46	−2.094	3.39	−2.077
PBE-D2	aDZ	3.63	−1.811	3.39	−2.274	3.32	−2.296
	aTZ	3.62	−1.852	3.40	−2.251	3.34	−2.251
PBE-D3	aDZ	3.81	−1.776	3.60	−2.231	3.52	−2.286
	aTZ	3.81	−1.805	3.61	−2.230	3.54	−2.278
M05-2X	aDZ	3.80	−1.129	3.55	−1.700	3.44	−1.782
	aTZ	3.80	−1.072	3.54	−1.560	3.47	−1.596
M06-2X	aDZ	3.65	−1.359	3.40	−2.205	3.31	−2.392
	aTZ	3.67	−1.273	3.38	−2.009	3.27	−2.149
ωB97X-D	aDZ	3.69	−1.888	3.45	−2.574	3.37	−2.671
	aTZ	3.70	−1.872	3.44	−2.476	3.37	−2.527
			CP-uncorrected				
B3LYP-D2	aDZ	3.55	−2.301	3.29	−2.931	3.22	−2.976
	aTZ	3.58	−1.910	3.34	−2.348	3.27	−2.361
B3LYP-D3	aDZ	3.68	−2.172	3.43	−2.729	3.37	−2.791
	aTZ	3.71	−1.826	3.48	−2.229	3.42	−2.261
B97-D2	aDZ	3.60	−2.278	3.37	−2.775	3.32	−2.824
	aTZ	3.65	−1.861	3.45	−2.188	3.38	−2.216
B97-D3	aDZ	3.66	−2.229	3.39	−2.768	3.33	−2.794
	aTZ	3.69	−1.829	3.45	−2.191	3.38	−2.189
PBE-D2	aDZ	3.57	−2.395	3.33	−2.970	3.26	−3.017
	aTZ	3.61	−1.958	3.39	−2.348	3.33	−2.366
PBE-D3	aDZ	3.74	−2.271	3.52	−2.803	3.46	−2.911
	aTZ	3.79	−1.898	3.60	−2.309	3.53	−2.375
M05-2X	aDZ	3.70	−1.755	3.44	−2.438	3.37	−2.582
	aTZ	3.79	−1.216	3.54	−1.694	3.45	−1.754
M06-2X	aDZ	3.58	−2.031	3.35	−2.988	3.26	−3.211
	aTZ	3.65	−1.445	3.37	−2.177	3.26	−2.335
ωB97X-D	aDZ	3.65	−2.419	3.41	−3.201	3.33	−3.336
	aTZ	3.69	−2.001	3.44	−2.596	3.36	−2.666

[a]The energy unit is 1 kcal/mol, and the distance unit is 1 Å.

fitting using the MOLPRO[64] code. A direct comparison of interaction energies between the two codes is difficult due to the different numerical grids employed. For benzene−methane and naphthalene−methane, a comparison of all DFT+D interaction energies between MOLPRO and Gaussian resulted in a MUE of 0.003 kcal/mol and a MeURE of 0.7%, well within acceptable precision.

Figures 7 and 8 show DFT+D and interaction-optimized density functional results, respectively, for the 3C naphthalene−methane complex. In addition, Table 4 collects the locations and depths of the naphthalene−methane minima for all three coordinations, with and without the CP correction, computed using all the DFT approaches tested. While the CP correction does not guarantee increased accuracy, especially in the DFT case, for all DFT+D methods this correction improved the agreement with the benchmark interaction potential, cf. Table 4. Therefore, only CP-corrected values are shown in Figure 7. It should be noted that the -D3 term can employ either the original damping function[19] that goes to zero at short interatomic distances or the Becke−Johnson damping whose short-range limit is a finite nonzero value.[104,105] Additionally, an inclusion of a three-body dispersion term has been suggested for large systems.[19] The resulting four variants of the -D3 correction are compared in Figure S5 in the Supporting Information for the benzene−methane and naphthalene−methane dimers. Neither the Becke−Johnson damping nor the three-body correction improve the results for the most accurate B3LYP-D3 and B97-D3 functionals. Therefore, the original -D3 variant is employed in Table 4, Figure 7, and throughout the rest of this work.

The results in Figures 7 and 8 and Table 4 show that the DFT+D methods generally capture the benchmark interaction

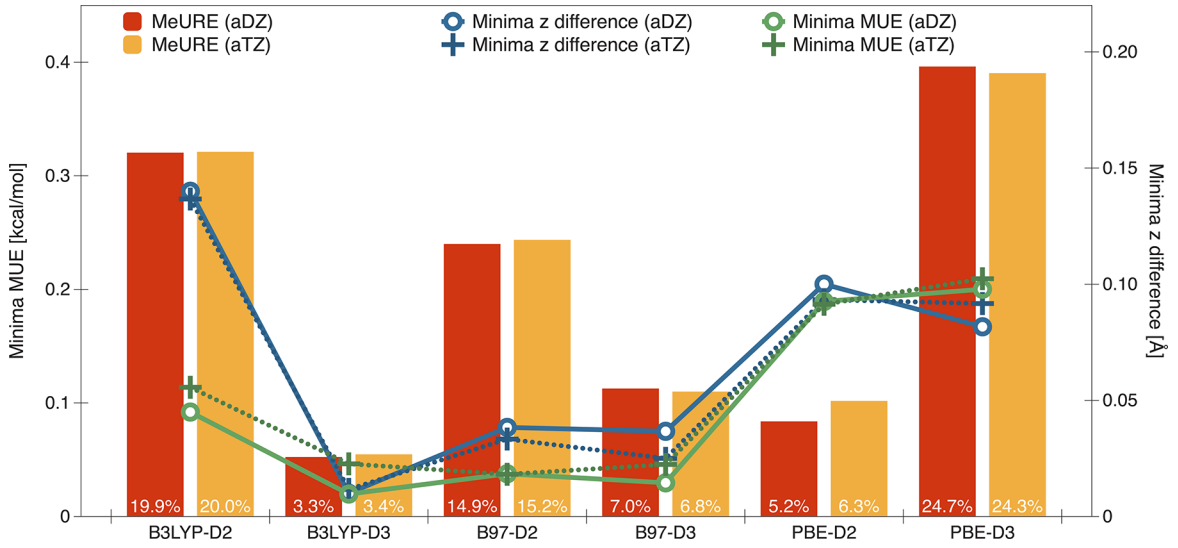

Figure 9. The values of the minima z differences, minima MUE, and MeURE, averaged over all six coordinations of the benzene−methane and naphthalene−methane complexes, for different CP-corrected DFT+D methods.

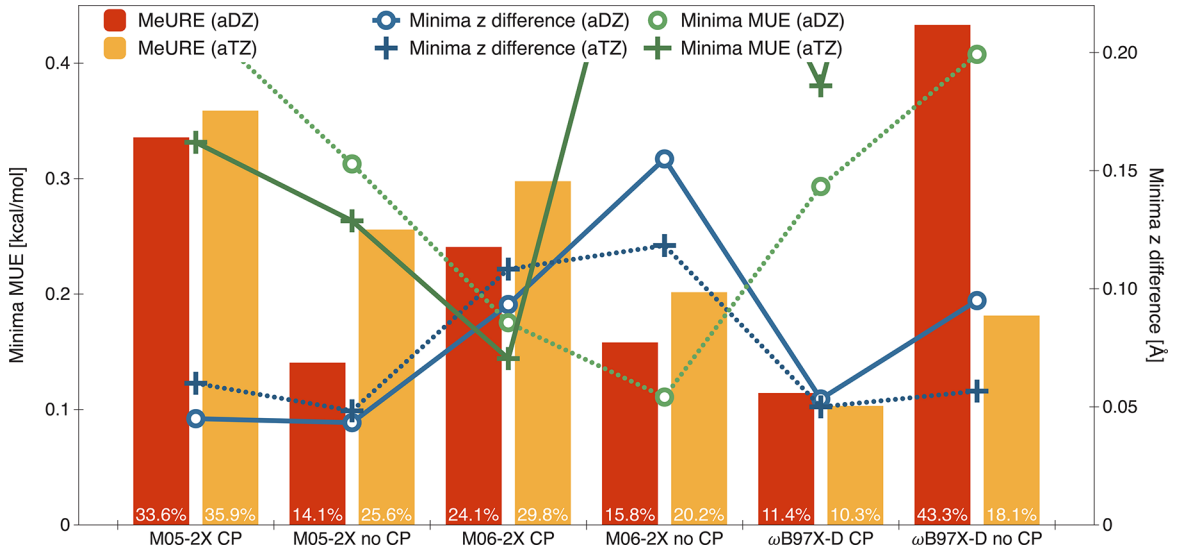

Figure 10. The values of the minima z differences, minima MUE, and MeURE, averaged over all six coordinations of the benzene−methane and naphthalene−methane complexes, for different interaction-optimized functionals (with and without the CP correction).

energy curve better than the interaction-optimized functionals. To quantify the performance of different DFT variants, the minima MUE, MeURE, and the mean minima z differences were computed for the six one-dimensional cuts for the benzene−methane and naphthalene−methane dimers. The pertinent results are shown in Figures 9 and 10 for DFT+D and interaction-optimized functionals, respectively. These figures show that the B3LYP-D3/aDZ approach offers the best performance in terms of all three statistical quantities, and the B3LYP-D3/aTZ, B97-D3/aDZ, and B97-D3/aTZ methods are not much worse. No interaction-optimized functional comes close to the accuracy of the best DFT+D variants for the PAH−methane dimers.

To assess the accuracy of different DFT+D methods for the anisotropy of the interaction energy, a one-dimensional angular cut through the benzene−methane potential energy surface was obtained by rotating the methane molecule around the carbon atom in such a way that the cut passes through all three coordinations of the system. To compare the anisotropy, the 1C structure was taken as the reference point, and energy differences with respect to this reference were compared against the benchmark. The three best DFT+D functionals in terms of MURE are B3LYP-D3/aDZ (0.5%), B97-D2/aTZ (0.5%), and B97-D3/aTZ (0.7%). The complete set of benchmark and DFT+D results for this angular cut is displayed in Figures S6−S7 in the Supporting Information.

Figure 11 demonstrates that the high accuracy of several DFT+D methods is retained for pyrene−methane (and, in fact, for all dimers up to this size). In order to identify the best DFT variant overall, Table 5 shows the three statistical quantities discussed above broken down into different coordinations for the three top performers. Note that, unlike in Figures 9 and 10, the averaging in Table 5 has been carried out over all the systems for which benchmark CCSD(T)-level potential energy curves are available, that is, benzene−methane through pyrene−methane. Table 5 demonstrates that B3LYP-D3/aDZ exhibits the best performance in nearly every category. On the basis of all the statistics presented above, we select the B3LYP-

dx.doi.org/10.1021/ct3008809 | J. Chem. Theory Comput. 2013, 9, 370−389

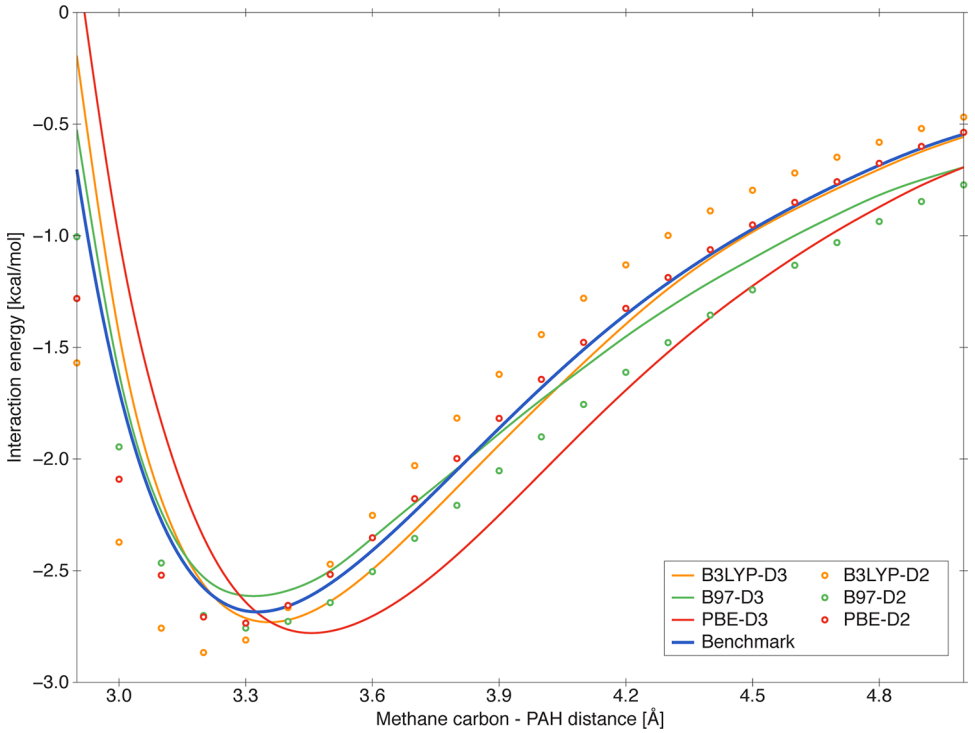

Figure 11. DFT+D/aTZ interaction potentials for the 3C pyrene−methane complex as compared to the MP2/(Q,5)+ΔCCSD(T)/aDZ benchmark.

Table 5. The Three Best DFT+D Functionals in Terms of MeURE Broken down into Different Coordinations of the Complexes[a]

	B3LYP-D3		B97-D3		PBE-D2	
	aDZ	aTZ	aDZ	aTZ	aDZ	aTZ
			minima z difference			
all	0.01	0.01	0.03	0.02	0.09	0.09
1C	0.01	0.01	0.02	0.03	0.09	0.10
2C	0.02	0.01	0.04	0.03	0.10	0.09
3C	0.01	0.01	0.03	0.01	0.09	0.07
			minima MUE			
all	0.039	0.072	0.041	0.060	0.151	0.140
1C	0.058	0.107	0.062	0.103	0.158	0.201
2C	0.041	0.070	0.035	0.031	0.157	0.133
3C	0.018	0.038	0.024	0.047	0.137	0.087
			MeURE			
all	2.52%	3.14%	7.01%	6.76%	3.86%	4.13%
1C	3.11%	3.93%	7.06%	6.98%	4.45%	6.20%
2C	2.73%	2.98%	7.20%	6.31%	4.01%	3.86%
3C	1.84%	2.35%	5.74%	7.21%	3.47%	3.04%

[a]The purpose of this breakdown is to illustrate that the lowest-energy structure of the complex is recovered better than the overall statistics suggest. The statistical averaging has been performed over all dimers from benzene−methane through pyrene−methane. The units are 1 Å for the minima z difference and 1 kcal/mol for the minima MUE.

D3/aDZ approach as the method of choice for larger systems, as coronene−methane is the last dimer for which CCSD(T) in any acceptable basis is feasible. It is also of interest that the DFT+D approach slightly overbinds the 1C and 2C structures, which lead to somewhat larger errors compared to the 3C configuration.

The 1C, 2C, and 3C minimum energies for the CCSD(T)/CBS benchmark, MP2/CBS, and the B3LYP-D3/aDZ functional for all dimers studied in this work are collected in Figure 6. The qualitative differences between the minima pattern for linear acenes and nonlinear PAHs are easily discernible at all levels of theory. Figure 6 demonstrates how the B3LYP-D3/aDZ approach performs remarkably well for all systems through pyrene−methane (in the worst case, the 1C pyrene−methane complex, the error is 0.110 kcal/mol or 6.2%) but overbinds the three coronene−methane minima by 0.126−0.292 kcal/mol or 4.2−13.9%. The accuracy of the B3LYP-D3/aDZ approach for coronene−methane is still quite good—for comparison, the MP2/CBS method overbinds the PAH−methane complexes by 30% and more. However, the increase in errors with respect to smaller complexes can be only partially explained by the increased uncertainty of the benchmark itself (due to the use of a reduced local-DZ basis for ΔCCSD(T) and the larger overall interaction energy) which is not expected to exceed 0.1 kcal/mol even for this system. It should be noted that B3LYP-D3/aDZ tends to overestimate the minimum energies more for the 1C and 2C configurations than for the 3C coordination. The second and third best performer overall, the B97-D3 and PBE-D2 functionals, are actually slightly more accurate than B3LYP-D3 for coronene−methane, cf. Table SVII in the Supporting Information. However, both functionals slightly underestimate the minimum intermolecular distances, while B3LYP-D3 is spot on in that respect.

To estimate the adsorption energy of methane on graphene and graphite, larger complexes are needed as there still is a large gap in interaction energy between pyrene−methane and coronene−methane. For systems larger than coronene−methane, the CCSD(T) calculations cannot be performed in a large enough basis set, and MP2 is deemed to overestimate the interaction energy considerably. Therefore, we resorted to the top DFT performer from our tests on smaller complexes, the B3LYP-D3 approach, to study the two largest complexes, hexabenzocoronene−methane and circumcoronene−methane (Figure 1). To find the minima for these systems, starting

intermolecular geometries were taken from the coronene−methane dimer, and then the B3LYP-D3/aDZ interaction energies were minimized in a three-dimensional search that disregarded methane rotation. The global-minimum interaction energies for the hexabenzocoronene−methane and circumcoronene−methane complexes are −3.214 and −3.362 kcal/mol, respectively. The latter result should be reasonably close to the graphene−methane interaction energy as the interactions with distant carbon atoms are not likely to change the interaction energy appreciably. Indeed, the addition of one and two additional rings of benzene rings around circumcoronene changes the -D3 empirical dispersion term by −0.087 and −0.118 kcal/mol, respectively, compared to circumcoronene−methane. At this range of distances, dispersion should constitute nearly 100% of interaction energy. Thus, our calculations predict that the minimum graphene−methane interaction energy is about −3.48 kcal/mol.

A direct comparison of the theoretical result to the experimental well depth of methane adsorbed on the (0001) surface of graphite[106] requires taking into account the interactions with the subsurface graphene sheets. To estimate the effect of the subsequent layers in graphite, a simple additive model is assumed where the contribution of each additional layer is estimated using the circumcoronene−methane model and the B3LYP-D3/aDZ approach. The distance between graphene layers in graphite is taken as 3.34 Å, and each layer is shifted by 1.43 Å with respect to the previous one to form an alternate ABAB... structure.[107] Starting with the methane−circumcoronene 3C global minimum geometry, in the models for subsequent layers the circumcoronene molecule is shifted in a way corresponding to the relative position of layers in graphite. The resulting B3LYP-D3 calculations give the adsorption energy contributions from the second, third, fourth, and fifth graphene layers equal to 0.200, 0.023, 0.006, and less than 0.001 kcal/mol, respectively. Thus, taking into account the first four layers, our final estimate of the methane adsorption energy on the (0001) graphite surface amounts to 3.71 kcal/mol. This value is somewhat larger than the experimental result of 2.99 ± 0.24 kcal/mol[106] and the DFT/CC result of 3.23 kcal/mol.[108] We will discuss this discrepancy in more detail in section 3.4.

3.3. SAPT(DFT) Calculations. To provide a better insight into the nature of the PAH−methane bonding and the effects determining the energetic ordering of different coordinations, we performed SAPT(DFT) calculations for several dimers along the same one-dimensional cuts through the potential energy surface as for the benchmark and DFT calculations. The total SAPT(DFT) interaction energies for the 2C and 3C configurations of naphthalene−methane are compared to the benchmark curves in Figure 12. An analogous figure for pyrene−methane is given in the Supporting Information. Figure 12 shows that the absolute accuracy of SAPT(DFT) is not very impressive—the depth of the global minimum is underestimated by 0.27 kcal/mol at the aTZ level. However, a substantial part of this discrepancy can be attributed to the basis set incompleteness effects as indicated by the SAPT(DFT)/aTZ minima being about 0.2 kcal/mol deeper than the SAPT(DFT)/aDZ ones. While SAPT(DFT) is not as accurate overall as the best DFT+D approaches for this system, Figure 12 demonstrates that it recovers the energy difference between the 2C and 3C configurations very well. Therefore, we can expect the SAPT(DFT) energy decomposition to provide reliable insight into the physical origin of interaction energy

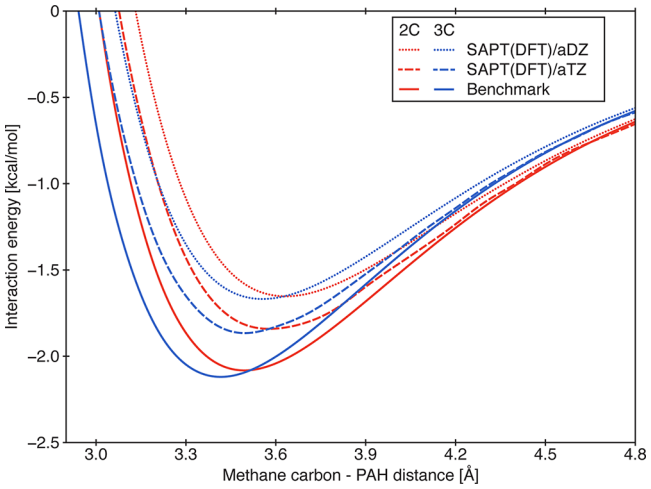

Figure 12. Total SAPT(DFT) interaction energies for the 2C and 3C naphthalene−methane configurations plotted against the benchmark data as functions of the intermolecular coordinate z.

differences between differently coordinated PAH−methane structures.

Table 6 shows the SAPT(DFT)/aDZ electrostatics, induction, dispersion, and first-order exchange contributions for the 2C and 3C minima of the naphthalene−methane and pyrene−methane dimers. It is clearly seen that both complexes, while primarily bound by dispersion, also contain a significant amount of attractive electrostatic interaction. While the latter interaction is nearly negligible in the asymptotic region (with the leading contribution coming from the quadrupole−octupole interaction), the charge overlap effects make it substantial in the region of the van der Waals minima. For the naphthalene−methane complex, the electrostatics and first-order exchange effects actually slightly favor the 2C configuration, but the 3C one exhibits more dispersion. As a result of a cancellation of these differences, the 2C and 3C minima are nearly isoenergetic just like we found for all other theory levels, cf. Figure 6. When the PAH is not a linear acene, such as in the pyrene−methane case, Figure 6 shows that the 3C minimum is significantly deeper than the 2C one. As the SAPT(DFT) contributions presented in Table 6 indicate, the 3C configuration exhibits stronger dispersion (and also somewhat stronger electrostatics) that more than makes up for the somewhat larger exchange repulsion compared to the 2C geometry. It is also worth noting that the differences between the SAPT(DFT) contributions for naphthalene−methane and pyrene−methane are much larger for the 3C geometry than for the 2C one. This behavior can be explained by the fact that an "extension" of naphthalene to pyrene for the 2C configuration involves adding atoms that are relatively far from the methane molecule and contribute little to the interaction energy, especially to the short-range first-order exchange part (cf. Figure 1). Conversely, a similar "extension" leading to 3C pyrene−methane involves creating a new aromatic ring directly below one of the methane hydrogens. This increases both the exchange repulsion and the attraction due to electrostatics and dispersion. The latter effect prevails and the 3C structure exhibits a significantly stronger bonding in the pyrene−methane complex than in the naphthalene−methane one.

3.4. Comparison to Other Work. The intermolecular separations z_{min} and interaction energies E_{int} at the global

dx.doi.org/10.1021/ct3008809 | J. Chem. Theory Comput. 2013, 9, 370−389

Table 6. Minimum Intermolecular Distances z_{min}, Interaction Energy Contributions, and Total Interaction Energies E_{int} Predicted by SAPT(DFT)/aDZ for the 2C and 3C Coordinations of Naphthalene−Methane and Pyrene−Methane As Compared to Benchmark[a]

	SAPT(DFT)						benchmark	
system	z_{min}	electrostatics	induction	dispersion	exchange	E_{int}	z_{min}	E_{int}
naphthalene−methane 2C	3.63	−0.834	−0.064	−2.914	2.160	−1.653	3.49	−2.082
naphthalene−methane 3C	3.55	−0.795	−0.060	−3.052	2.239	−1.668	3.41	−2.119
pyrene−methane 2C	3.61	−0.802	−0.051	−3.262	2.248	−1.867	3.47	−2.362
pyrene−methane 3C	3.47	−0.950	−0.049	−3.694	2.590	−2.103	3.33	−2.678

[a]The energy unit is 1 kcal/mol, and the distance unit is 1 Å.

Table 7. Global Minimum Methane Carbon−PAH Plane Separations z_{min} (in Å) and Interaction Energies E_{int} (in kcal/mol) for All Complexes Investigated in the Present Work Compared to Previous Theoretical and Experimental Studies[a]

			this work		other works	
system		theory level	z_{min}	E_{int}	z_{min}	E_{int}
benzene−methane	1C	MP2-F12/(Q,5)+ΔCCSD(T)-F12b/(T,Q)	3.76	−1.433	3.72 [33]	−1.50 [33],[e] −1.448 [39, 41][f] −1.438 [75][g]
naphthalene−methane	3C	MP2/(Q,5)+ΔCCSD(T)-F12b/(D,T)	3.41	−2.119	3.6 [58]	−1.92 [58][h]
antracene-methane	3C	MP2/(Q,5)+ΔCCSD(T)/aDZ	3.40	−2.258		
tetracene-methane	3C	MP2/(Q,5)+ΔCCSD(T)/aDZ	3.40	−2.359		
phenanthrene-methane	3C	MP2/(Q,5)+ΔCCSD(T)/aDZ	3.38	−2.378		
pyrene−methane	3C	MP2/(Q,5)+ΔCCSD(T)/aDZ	3.33	−2.678	3.4 [58], 3.36 [110]	−2.50 [58],[h] −2.91 [110][i]
coronene−methane	3C	MP2/(T,Q)+ΔCCSD(T)/local-DZ	3.32	−2.849	3.31 [108], 3.37 [110]	−2.799 [108],[j] −3.32 [110][i]
hexabenzocoronene−methane	3C	B3LYP-D3/aDZ	3.32	−3.214		
circumcoronene−methane	3C	B3LYP-D3/aDZ	3.32	−3.362		
graphene-methane	3C	est. B3LYP-D3/aDZ	3.32[b]	3.48[c]	3.31 [108], 3.28 [109]	3.23 [108],[k] 3.92 [109][l]
graphite-methane	3C	est. B3LYP-D3/aDZ	3.32[b]	3.71[d]	3.03−3.45 [106]	2.99 ± 0.24 [106][m]

[a]Different estimates of the adsorption energy of methane on graphene and (0001) graphite are also given. The reference numbers for literature values are given in square brackets. [b]Taken from the circumcoronene−methane calculation. [c]The circumcoronene−methane result plus the -D3 correction for interaction with distant carbon atoms. [d]The graphene−methane result plus a B3LYP-D3/aDZ estimate of the contribution from subsurface graphene layers. [e]Original S22 database: MP2/cc-pVTZ optimized geometry, MP2/(cc-pVQZ,cc-pV5Z)+ΔCCSD(T)/(reduced cc-pVTZ) energy. [f]Revised S22 database: MP2/(Q,5)+ΔCCSD(T)/(aTZ+midbond) energy at the geometry from ref 33. [g]CCSD(T)/(heavy-TZ,heavy-QZ). [h]MP2(cc-pVDZ,cc-pVTZ)+ΔCCSD(T)/6-31G* energy at the MP2/6-31G*(0.25) optimized geometry. [i]BLYP-D3/aTZ. [j]DFT/CC using the PBE functional and the aQZ basis. [k]Periodic DFT/CC using the PBE functional and a plane-wave basis. [l]MP2/aTZ. [m]Experiment.

minima for all dimers considered in this work, including the estimates of the adsorption energy of methane on graphene and graphite, are collected in Table 7 and compared to the most accurate literature results. It should be noted that, in a few cases, different minimum structures were found in the previous studies. Specifically, Tsuzuki et al. found,[58] through an MP2/6-31G*(0.25) geometry optimization, a naphthalene−methane minimum structure that is an intermediate between the 2C and 3C ones (closer to the 2C configuration). The ordering of the minima found by Thierfelder et al.[109] for graphene−methane (using MP2 for a finite cluster and periodic DFT for an infinite sheet) varies with the method and density functional employed. Finally, Qiu et al.[110] considered nine different structures of coronene−methane, but neither of them corresponds to the global minimum located in this work. The lowest-energy structure of ref 110, a 3C configuration but with the methane carbon placed over the center of the inner coronene ring, exhibits an interaction energy (minimized with respect to the z distance) of −2.686 kcal/mol at the MP2(T,Q)+ΔCCSD(T)/local-DZ level, 0.162 kcal/mol above the global minimum.

The first system in Table 7, the benzene−methane complex, has been the subject of numerous high-level *ab initio* studies.[33,34,38−40,75,111] The present work is the only one where the CCSD(T) interaction energy was computed in a fully augmented quadruple-ζ basis set (although Marchetti and Werner[75] used heavy-QZ) so that our result is theoretically the most accurate. However, the most accurate previous results were already well converged, so the improvement is very modest. On the contrary, the only CCSD(T) interaction energies available for larger PAH−methane dimers, the results of Tsuzuki et al.[58] for naphthalene−methane and pyrene−methane, are underestimated by about 0.2 kcal/mol. Obviously, the small 6-31G* basis used to compute ΔCCSD(T) in ref 58 is far from complete.

The BLYP-D3 pyrene−methane and coronene−methane interaction energies from ref 110 are overestimated by 0.23 and 0.47 kcal/mol, respectively, relative to our benchmarks. Clearly, the performance of BLYP-D3 is not competitive with that of the best DFT+D variants tested in this work, most notably B3LYP-D3 (cf. the minima MUE values in Table 5). On the other hand, the excellent agreement (to 0.05 kcal/mol) of our coronene−methane result with the DFT/CC one of Rubeš et al.[108] provides a strong validation of the assumption that the differences between CCSD(T) and DFT, computed for small dimers, are transferable to larger PAH−methane complexes (note the agreement between the minimum geometries too). This underlying assumption of the DFT/CC approach is also employed by us to justify the selection of an optimal DFT+D variant for large systems via a comparison to benchmark small-system CCSD(T) interaction energies.

As far as the methane adsorption energy on infinite carbon structures is concerned, the review work of Vidali et al.[106]

recommended, based on a number of experimental studies, the value of 2.99 ± 0.24 kcal/mol as the zero-coverage adsorption well depth of methane on the (0001) surface of graphite and 3.24 ± 0.21 Å as the distance between the methane carbon and the surface. While all computational studies give adsorption distances within the broad experimental range, the same is not true for the adsorption energy. The periodic DFT/CC result of Rubeš et al.[108] is at the upper end of the experimental range while our estimate, although certainly more accurate than the MP2 one of ref 109, is 0.48 kcal/mol above the higher experimental limit. The reason for this discrepancy is that the B3LYP-D3/aDZ approach employed by us somewhat overestimates the global-minimum interaction energies (cf. Figure 6). The extent of this overestimation has been observed to increase between pyrene−methane and coronene−methane (from 0.033 to 0.126 kcal/mol), and it is likely that this trend continues to circumcoronene−methane. In that case, the B97-D3/aDZ approach, which overestimates the coronene−methane global-minimum interaction energy by only 0.053 kcal/mol, might accidentally be a better choice for extended systems even though it is inferior to B3LYP-D3 for the description of the entire potential energy curve (as indicated by the larger MeURE values in Figure 9 and Table 5). The B97-D3/aDZ circumcoronene−methane interaction energy amounts to −3.217 kcal/mol for the z distance of 3.32 Å. If this result is augmented with the corrections for the more distant carbon atoms in the first graphene sheet and the subsurface graphene layers, the resulting B97-D3/aDZ estimate of the methane adsorption energy on graphite amounts to 3.58 kcal/mol, less than for B3LYP-D3/aDZ but still outside the experimental range. Finally, let us note that if the graphene−methane result of Rubeš et al.[108] is augmented by our estimate of the contributions from subsurface graphene layers (neglected in ref 108), the resulting adsorption energy of 3.46 kcal/mol is also above the upper experimental limit. Thus, it is possible that the experimental value is somewhat underestimated and the deviation of our B3LYP-D3/aDZ result from the true adsorption energy is no more than 0.2 kcal/mol.

4. SUMMARY

High-accuracy benchmark interaction energies were obtained for weakly interacting complexes of aromatic hydrocarbons (benzene, naphthalene, anthracene, phenanthrene, tetracene, pyrene, and coronene) with methane. The energies were computed by the supermolecular MP2 approach extrapolated to the complete basis set limit plus a CCSD(T) correction calculated in a moderate basis set (up to aQZ for benzene−methane, aTZ for naphthalene−methane, aDZ for anthracene−methane through pyrene−methane, and local-DZ for coronene−methane). The calculations for benzene−methane and naphthalene−methane utilized the explicitly correlated CCSD(T)-F12a/b approach while all other systems were treated using conventional CCSD(T). An extensive basis set convergence analysis indicates that our benchmark interaction energies are accurate to a few hundredths of a kilocalorie per mole.

Our CCSD(T) results indicate that the very well studied benzene−methane complex is not at all representative of the interactions between methane and larger PAHs. The benzene−methane global minimum is singly coordinated (1C); that is, only one methane hydrogen points toward the benzene plane. For all other complexes (that have not been studied at the CCSD(T) level before except for the very small-basis work of Tsuzuki et al.[58]), the 1C structure is significantly less bound than the 2C and 3C ones. The global minimum for naphthalene−methane and all larger complexes is triply coordinated; however, the linear and nonlinear PAHs lead to a qualitatively different behavior. In the nonlinear case, the 3C structure is highly favored over all others as, except for the phenanthrene complex, all three hydrogens can be placed on top of different aromatic rings. Such a placement is not possible for linear acenes: as a result, the 2C and 3C minima are nearly isoenergetic in this case. The binding patterns between methane and PAHs can be understood in terms of a competition between dispersion, exchange repulsion, and electrostatics as illustrated by the SAPT(DFT) decomposition of the interaction energy performed for selected dimers.

The CCSD(T)-level benchmarks developed here were used to investigate the accuracy of several novel DFT approaches for the PAH−methane interaction energies. The comparisons included one-dimensional cuts through the PAH−methane potential energy surfaces passing through the deepest minima in each of the three coordinations. Thus, the optimal DFT variant needs to provide a uniformly high accuracy for all intermolecular distances, not just around the van der Waals minima. The tested approaches included DFT+D (with the B3LYP, PBE, and Grimme's reparameterization of B97[12] as the density functionals and Grimme's -D2[12] and -D3[19] empirical corrections for dispersion) and functionals specifically optimized for weak intermolecular interactions (M05-2X, M06-2X, and ωB97X-D). While the latter group of functionals somewhat underperformed for the complexes studied here, the DFT+D approach, employing the aDZ and aTZ basis sets and including the counterpoise correction, reproduced the benchmark results very well. The accuracy of the CP-corrected B3LYP-D3/aDZ method was particularly remarkable and consistent across different dimers (benzene−methane through pyrene−methane), coordinations, and distances, with an overall mean unsigned error at the minima equal to 0.039 kcal/mol and a median unsigned relative error for all points amounting to 2.52%. The B3LYP-D3 functional performed similarly well in the aTZ basis set, and the B97-D3 approach came a close second. The accuracy of the B3LYP-D3/aDZ method somewhat deteriorated for the coronene−methane complex, but the global minimum was still reproduced to within 0.13 kcal/mol.

The excellent reproduction of benchmark results with the B3LYP-D3 approach suggests that it should be the method of choice for studying interactions of methane with larger PAHs as well as with extended structures such as graphene sheets and carbon nanotubes. We performed the first step in this direction and computed B3LYP-D3/aDZ interaction energies for the three coordinations of hexabenzocoronene−methane and circumcoronene−methane. Compared to the coronene−methane dimer, the presence of an additional outer ring of benzene rings increases the binding by about 0.5 kcal/mol. As the main binding force is provided by dispersion, an extension of the PAH beyond circumcoronene results in a small change in the interaction energy and can be modeled by the empirical dispersion term alone. The inclusion of the effect of this extension and of the contribution from the subsequent layers leads to estimated methane adsorption energies on graphite equal to 3.71 (B3LYP-D3) and 3.58 (B97-D3) kcal/mol, close to the experimental value but above its upper limit. A similar estimate of the adsorption energy of methane on the inner and outer surfaces of a carbon nanotube needs to take into account,

in addition to all other effects, the nanotube curvature. Further work in this direction is in progress in our group.

■ ASSOCIATED CONTENT

Supporting Information

Additional CCSD(T)-F12 results for benzene−methane (Table SI), potential minima for all systems and density functionals (Tables SII−SVII), benchmark interaction potentials for all systems (Figures S1−S4), comparison of different -D3 variants (Figure S5), anisotropy of the benzene−methane potential (Figures S6−S7), and SAPT(DFT) curves for pyrene−methane (Figure S8). This information is available free of charge via the Internet at http://pubs.acs.org/.

■ AUTHOR INFORMATION

Corresponding Author

*E-mail: patkowsk@auburn.edu.

Notes

The authors declare no competing financial interest.

■ ACKNOWLEDGMENTS

This research was supported by the Donors of the American Chemical Society Petroleum Research Fund and by the startup funding from Auburn University. Some of the calculations were performed at the Alabama Supercomputer Center.

■ REFERENCES

(1) Chałasiński, G.; Szczęśniak, M. M. *Chem. Rev.* **2000**, *100*, 4227−4252.
(2) Halkier, A.; Helgaker, T.; Jørgensen, P.; Klopper, W.; Koch, H.; Olsen, J.; Wilson, A. K. *Chem. Phys. Lett.* **1998**, *286*, 243−252.
(3) Schwenke, D. W. *J. Chem. Phys.* **2005**, *122*, 014107.
(4) Tao, F.-M.; Pan, Y.-K. *J. Chem. Phys.* **1991**, *95*, 3582−3588.
(5) Hättig, C.; Klopper, W.; Köhn, A.; Tew, D. P. *Chem. Rev.* **2012**, *112*, 4−74.
(6) Kong, L.; Bischoff, F. A.; Valeev, E. F. *Chem. Rev.* **2012**, *112*, 75−107.
(7) Patkowski, K.; Podeszwa, R.; Szalewicz, K. *J. Phys. Chem. A* **2007**, *111*, 12822−12838.
(8) Peréz-Jordá, J. M.; Becke, A. D. *Chem. Phys. Lett.* **1995**, *233*, 134−137.
(9) Wu, X.; Vargas, M. C.; Nayak, S.; Lotrich, V. F.; Scoles, G. *J. Chem. Phys.* **2001**, *115*, 8748−8757.
(10) Wu, Q.; Yang, W. *J. Chem. Phys.* **2002**, *116*, 515−524.
(11) Dion, M.; Rydberg, H.; Schröder, E.; Langreth, D. C.; Lundqvist, B. I. *Phys. Rev. Lett.* **2004**, *92*, 246401.
(12) Grimme, S. *J. Comput. Chem.* **2006**, *27*, 1787−1799.
(13) Zhao, Y.; Schultz, N. E.; Truhlar, D. G. *J. Chem. Theory Comput.* **2006**, *2*, 364−382.
(14) Becke, A. D.; Johnson, E. R. *J. Chem. Phys.* **2007**, *127*, 124108.
(15) Chai, J.-D.; Head-Gordon, M. *Phys. Chem. Chem. Phys.* **2008**, *10*, 6615−6620.
(16) Zhao, Y.; Truhlar, D. G. *Theor. Chem. Acc.* **2008**, *120*, 215−241.
(17) Tkatchenko, A.; Scheffler, M. *Phys. Rev. Lett.* **2009**, *102*, 073005.
(18) Pernal, K.; Podeszwa, R.; Patkowski, K.; Szalewicz, K. *Phys. Rev. Lett.* **2009**, *103*, 263201.
(19) Grimme, S.; Antony, J.; Ehrlich, S.; Krieg, H. *J. Chem. Phys.* **2010**, *132*, 154104.
(20) Steinmann, S. N.; Corminboeuf, C. *J. Chem. Theory Comput.* **2010**, *6*, 1990−2001.
(21) Vydrov, O. A.; Van Voorhis, T. *J. Chem. Phys.* **2010**, *133*, 244103.
(22) Grimme, S. *J. Chem. Phys.* **2003**, *118*, 9095−9102.
(23) Hill, J. G.; Platts, J. A. *J. Chem. Theory Comput.* **2007**, *3*, 80−85.
(24) DiStasio, R. A., Jr.; Head-Gordon, M. *Mol. Phys.* **2007**, *105*, 1073−1083.
(25) Takatani, T.; Hohenstein, E. G.; Sherrill, C. D. *J. Chem. Phys.* **2008**, *128*, 124111.
(26) Pitoňák, M.; Neogrady, P.; Černý, J.; Grimme, S.; Hobza, P. *ChemPhysChem* **2009**, *10*, 282−289.
(27) Misquitta, A. J.; Podeszwa, R.; Jeziorski, B.; Szalewicz, K. *J. Chem. Phys.* **2005**, *123*, 214103.
(28) Hesselmann, A.; Jansen, G.; Schütz, M. *J. Chem. Phys.* **2005**, *122*, 014103.
(29) Hesselmann, A. *J. Chem. Phys.* **2008**, *128*, 144112.
(30) Bludský, O.; Rubeš, M.; Soldán, P.; Nachtigall, P. *J. Chem. Phys.* **2008**, *128*, 114102.
(31) Zhao, Y.; Truhlar, D. G. *J. Chem. Theory Comput.* **2005**, *1*, 415−432.
(32) Zhao, Y.; Truhlar, D. G. *J. Phys. Chem. A* **2005**, *109*, 5656−5667.
(33) Jurečka, P.; Šponer, J.; Černý, J.; Hobza, P. *Phys. Chem. Chem. Phys.* **2006**, *8*, 1985−1993.
(34) Sherrill, C. D.; Takatani, T.; Hohenstein, E. G. *J. Phys. Chem. A* **2009**, *113*, 10146−10159.
(35) Gráfová, L.; Pitoňák, M.; Řezáč, J.; Hobza, P. *J. Chem. Theory Comput.* **2010**, *6*, 2365−2376.
(36) Thanthiriwatte, K. S.; Hohenstein, E. G.; Burns, L. A.; Sherrill, C. D. *J. Chem. Theory Comput.* **2011**, *7*, 88−96.
(37) Řezáč, J.; Riley, K. E.; Hobza, P. *J. Chem. Theory Comput.* **2011**, *7*, 2427−2438.
(38) Marchetti, O.; Werner, H. *Phys. Chem. Chem. Phys.* **2008**, *10*, 3400−3409.
(39) Podeszwa, R.; Patkowski, K.; Szalewicz, K. *Phys. Chem. Chem. Phys.* **2010**, *12*, 5974−5979.
(40) Takatani, T.; Hohenstein, E. G.; Malagoli, M.; Marshall, M. S.; Sherrill, C. D. *J. Chem. Phys.* **2010**, *132*, 144104.
(41) Marshall, M. S.; Burns, L. A.; Sherrill, C. D. *J. Chem. Phys.* **2011**, *135*, 194102.
(42) Burns, L. A.; Vazquez-Mayagoitia, A.; Sumpter, B. G.; Sherrill, C. D. *J. Chem. Phys.* **2011**, *134*, 084107.
(43) Novoselov, K. S.; Geim, A. K.; Morozov, S. V.; Jiang, D.; Zhang, Y.; Dubonos, S. V.; Grigorieva, I. V.; Firsov, A. A. *Science* **2004**, *306*, 666−669.
(44) Iijima, S. *Nature* **1991**, *354*, 56−58.
(45) Britz, D. A.; Khlobystov, A. N. *Chem. Soc. Rev.* **2006**, *35*, 637−659.
(46) Dillon, A. C.; Jones, K. M.; Bekkedahl, T. A.; Kiang, C. H.; Bethune, D. S.; Heben, M. J. *Nature* **1997**, *386*, 377−379.
(47) Kong, J.; Franklin, N. R.; Zhou, C. W.; Chapline, M. G.; Peng, S.; Cho, K. J.; Dai, H. J. *Science* **2000**, *287*, 622−625.
(48) Duren, T.; Sarkisov, L.; Yaghi, O. M.; Snurr, R. Q. *Langmuir* **2004**, *20*, 2683−2689.
(49) Bruch, L. W.; Diehl, R. D.; Venables, J. A. *Rev. Mod. Phys.* **2007**, *79*, 1381−1454.
(50) Murdachaew, G.; de Gironcoli, S.; Scoles, G. *J. Phys. Chem. A* **2008**, *112*, 9993−10005.
(51) Becke, A. D. *J. Chem. Phys.* **1993**, *98*, 5648−5652.
(52) Stephens, P. J.; Devlin, F. J.; Chabalowski, C. F.; Frisch, M. J. *J. Phys. Chem.* **1994**, *98*, 11623−11627.
(53) Perdew, J. P.; Burke, K.; Ernzerhof, M. *Phys. Rev. Lett.* **1996**, *77*, 3865−3868.
(54) Yang, S.; Ouyang, L.; Phillips, J. M.; Ching, W. Y. *Phys. Rev. B* **2006**, *73*, 165407.
(55) Albesa, A. G.; Fertitta, E. A.; Vicente, J. L. *Langmuir* **2010**, *26*, 786−795.
(56) Liu, Y. Y.; Wilcox, J. *Environ. Sci. Technol.* **2011**, *45*, 809−814.
(57) Wong, B. M. *J. Comput. Chem.* **2009**, *30*, 51−56.
(58) Tsuzuki, S.; Honda, K.; Fujii, A.; Uchimaru, T.; Mikami, M. *Phys. Chem. Chem. Phys.* **2008**, *10*, 2860−2865.
(59) Dunning, T. H., Jr. *J. Chem. Phys.* **1989**, *90*, 1007−1023.
(60) Špirko, V.; Rubeš, M.; Bludský, O. *J. Chem. Phys.* **2010**, *132*, 194708.
(61) Jenness, G. R.; Karalti, O.; Jordan, K. D. *Phys. Chem. Chem. Phys.* **2010**, *12*, 6375−6381.

(62) Hachmann, J.; Dorando, J. J.; Avilés, M.; Chan, G. K.-L. *J. Chem. Phys.* **2007**, *127*, 134309.
(63) Janssen, C. L.; Nielsen, I. M. B. *Chem. Phys. Lett.* **1998**, *290*, 423−430.
(64) Werner, H. J.; Knowles, P. J.; Knizia, G.; Manby, F. R.; Schütz, M.; Celani, P.; Korona, T.; Lindh, R.; Mitrushenkov, A.; Rauhut, G.; Shamasundar, K. R.; Adler, T. B.; Amos, R. D.; Bernhardsson, A.; Berning, A.; Cooper, D. L.; Deegan, M. J. O.; Dobbyn, A. J.; Eckert, F.; Goll, E.; Hampel, C.; Hesselmann, A.; Hetzer, G.; Hrenar, T.; Jansen, G.; Köppl, C.; Liu, Y.; Lloyd, A. W.; Mata, R. A.; May, A. J.; McNicholas, S. J.; Meyer, W.; Mura, M. E.; Nicklass, A.; O'Neill, D. P.; Palmieri, P.; Pflüger, K.; Pitzer, R.; Reiher, M.; Shiozaki, T.; Stoll, H.; Stone, A. J.; Tarroni, R.; Thorsteinsson, T.; Wang, M.; Wolf, A. *MOLPRO*, version 2010.1; Cardiff University: Cardiff, U. K.; Universität Stuttgart: Stuttgart, Germany, 2010. See http://www.molpro.net (accessed Nov 6, 2012).
(65) Werner, H.-J.; Manby, F. R.; Knowles, P. J. *J. Chem. Phys.* **2003**, *118*, 8149−8160.
(66) Kendall, R. A.; Dunning, T. H., Jr.; Harrison, R. J. *J. Chem. Phys.* **1992**, *96*, 6796−6806.
(67) Weigend, F.; Köhn, A.; Hättig, C. *J. Chem. Phys.* **2002**, *116*, 3175−3183.
(68) Hättig, C. *Phys. Chem. Chem. Phys.* **2005**, *7*, 59−66.
(69) Boys, S. F.; Bernardi, F. *Mol. Phys.* **1970**, *19*, 553−566.
(70) van Duijneveldt, F. B.; van Duijneveldt-van de Rijdt, J. G. C. M.; van Lenthe, J. H. *Chem. Rev.* **1994**, *94*, 1873−1885.
(71) Adler, T. B.; Knizia, G.; Werner, H.-J. *J. Chem. Phys.* **2007**, *127*, 221106.
(72) Knizia, G.; Adler, T. B.; Werner, H.-J. *J. Chem. Phys.* **2009**, *130*, 054104.
(73) Köhn, A. *J. Chem. Phys.* **2009**, *130*, 131101.
(74) Tew, D. P.; Klopper, W.; Hättig, C. *Chem. Phys. Lett.* **2008**, *452*, 326−332.
(75) Marchetti, O.; Werner, H.-J. *J. Phys. Chem. A* **2009**, *113*, 11580−11585.
(76) McMahon, J. D.; Lane, J. R. *J. Chem. Phys.* **2011**, *135*, 154309.
(77) Patkowski, K. *J. Chem. Phys.* **2012**, *137*, 034103.
(78) Marshall, M. S.; Sherrill, C. D. *J. Chem. Theory Comput.* **2011**, *7*, 3978−3982.
(79) Becke, A. D. *J. Chem. Phys.* **1997**, *107*, 8554−8560.
(80) Weigend, F. *Phys. Chem. Chem. Phys.* **2002**, *4*, 4285−4291.
(81) Frisch, M. J.; Trucks, G. W.; Schlegel, H. B.; Scuseria, G. E.; Robb, M. A.; Cheeseman, J. R.; Scalmani, G.; Barone, V.; Mennucci, B.; Petersson, G. A.; Nakatsuji, H.; Caricato, M.; Li, X.; Hratchian, H. P.; Izmaylov, A. F.; Bloino, J.; Zheng, G.; Sonnenberg, J. L.; Hada, M.; Ehara, M.; Toyota, K.; Fukuda, R.; Hasegawa, J.; Ishida, M.; Nakajima, T.; Honda, Y.; Kitao, O.; Nakai, H.; Vreven, T.; Montgomery, J. A., Jr.; Peralta, J. E.; Ogliaro, F.; Bearpark, M.; Heyd, J. J.; Brothers, E.; Kudin, K. N.; Staroverov, V. N.; Kobayashi, R.; Normand, J.; Raghavachari, K.; Rendell, A.; Burant, J. C.; Iyengar, S. S.; Tomasi, J.; Cossi, M.; Rega, N.; Millam, J. M.; Klene, M.; Knox, J. E.; Cross, J. B.; Bakken, V.; Adamo, C.; Jaramillo, J.; Gomperts, R.; Stratmann, R. E.; Yazyev, O.; Austin, A. J.; Cammi, R.; Pomelli, C.; Ochterski, J. W.; Martin, R. L.; Morokuma, K.; Zakrzewski, V. G.; Voth, G. A.; Salvador, P.; Dannenberg, J. J.; Dapprich, S.; Daniels, A. D.; Farkas, O.; Foresman, J. B.; Ortiz, J. V.; Cioslowski, J.; Fox, D. J. *Gaussian 09*, revision A.1. Gaussian Inc.: Wallingford, CT, 2009.
(82) Vosko, S. H.; Wilk, L.; Nusair, M. *Can. J. Phys.* **1980**, *58*, 1200.
(83) Johnson, E. R.; Becke, A. D.; Sherrill, C. D.; DiLabio, G. A. *J. Chem. Phys.* **2009**, *131*, 034111.
(84) Adamo, C.; Barone, V. *J. Chem. Phys.* **1999**, *110*, 6158−6170.
(85) DALTON, a molecular electronic structure program, release 2.0 (2005). See http://daltonprogram.org (accessed Nov 6, 2012).
(86) Bukowski, R.; Cencek, W.; Jankowski, P.; Jeziorska, M.; Jeziorski, B.; Kucharski, S. A.; Lotrich, V. F.; Misquitta, A. J.; Moszyński, R.; Patkowski, K.; Podeszwa, R.; Rybak, S.; Szalewicz, K.; Williams, H. L.; Wheatley, R. J.; Wormer, P. E. S.; Żuchowski, P. S. *SAPT2008*; University of Delaware: Newark, DE; University of Warsaw: Warsaw, Poland (http://www.physics.udel.edu/~szalewic/SAPT/SAPT.html, accessed Nov 6, 2012).
(87) Tozer, D. J.; Handy, N. C. *J. Chem. Phys.* **1998**, *109*, 10180−10189.
(88) Lias, S. G. *Ionization Energy Evaluation, in NIST Chemistry WebBook, NIST Standard Reference Database Number 69*; Linstrom, P. J., Mallard, W. G., Eds.; National Institute of Standards and Technology: Gaithersburg MD. http://webbook.nist.gov (accessed Nov 6, 2012).
(89) Patkowski, K.; Szalewicz, K.; Jeziorski, B. *J. Chem. Phys.* **2006**, *125*, 154107.
(90) Patkowski, K.; Szalewicz, K.; Jeziorski, B. *Theor. Chem. Acc.* **2010**, *127*, 211−221.
(91) Zhao, Y.; Truhlar, D. G. *J. Phys. Chem. A* **2006**, *110*, 5121−5129.
(92) Podeszwa, R.; Szalewicz, K. *J. Chem. Phys.* **2012**, *136*, 161102.
(93) Yoo, S.; Aprà, E.; Zeng, X. C.; Xantheas, S. S. *J. Phys. Chem. Lett.* **2010**, *1*, 3122−3127.
(94) Ziółkowski, M.; Jansík, B.; Kjærgaard, T.; Jørgensen, P. *J. Chem. Phys.* **2010**, *133*, 014107.
(95) Janowski, T.; Pulay, P.; Karunarathna, A. A. S.; Sygula, A.; Saebø, S. *Chem. Phys. Lett.* **2011**, *512*, 155−160.
(96) Sullivan, M. B.; Iron, M. A.; Redfern, P. C.; Martin, J. M. L.; Curtiss, L. A.; Radom, L. *J. Phys. Chem. A* **2003**, *107*, 5617−5630.
(97) Sinnokrot, M. O.; Sherrill, C. D. *J. Phys. Chem. A* **2004**, *108*, 10200−10207.
(98) Papajak, E.; Zheng, J.; Xu, X.; Leverentz, H. R.; Truhlar, D. G. *J. Chem. Theory Comput.* **2011**, *7*, 3027−3034.
(99) ElSohly, A.; Tschumper, S. *Int. J. Quantum Chem.* **2009**, *109*, 91−96.
(100) Papajak, E.; Leverentz, H. R.; Zheng, J.; Truhlar, D. G. *J. Chem. Theory Comput.* **2009**, *5*, 1197−1202.
(101) Pitoňák, M.; Neogrády, P.; Řezáč, J.; Jurečka, P.; Urban, M.; Hobza, P. *J. Chem. Theory Comput.* **2008**, *4*, 1829−1834.
(102) Kucharski, S. A.; Bartlett, R. J. *J. Chem. Phys.* **1998**, *108*, 9221−9226.
(103) Stanton, J.; Gauss, J.; Harding, M.; Szalay, P.; Auer, A.; Bartlett, R.; Benedikt, U.; Berger, C.; Bernholdt, D.; Bomble, Y.; Christiansen, O.; Heckert, M.; Heun, O.; Huber, C.; Jagau, T.-C. et al. *CFOUR*, a quantum chemical program package, containing the integral packages MOLECULE (Almlöf, J.; Taylor, P. R.), PROPS (Taylor, P. R.), ABACUS (Helgaker, T.; Jensen, H. J. Aa.; Jørgensen, P.; Olsen, J.), and ECP routines (Mitin, A. V.; van Wüllen, C.). For the current version, see http://www.cfour.de (accessed Nov 6, 2012).
(104) Johnson, E. R.; Becke, A. D. *J. Chem. Phys.* **2005**, *123*, 024101.
(105) Grimme, S.; Ehrlich, S.; Goerigk, L. *J. Comput. Chem.* **2011**, *32*, 1456−1465.
(106) Vidali, G.; Ihm, G.; Kim, H. Y.; Cole, M. W. *Surf. Sci. Rep.* **1991**, *12*, 135−181.
(107) Podeszwa, R. *J. Chem. Phys.* **2010**, *132*, 044704.
(108) Rubeš, M.; Kysilka, J.; Nachtigall, P.; Bludský, O. *Phys. Chem. Chem. Phys.* **2010**, *12*, 6438−6444.
(109) Thierfelder, C.; Witte, M.; Blankenburg, S.; Rauls, E.; Schmidt, W. G. *Surf. Sci.* **2011**, *605*, 746−749.
(110) Qiu, N.-X.; Xue, Y.; Guo, Y.; Sun, W.-J.; Chu, W. *Comp. Theor. Chem.* **2012**, *992*, 37−47.
(111) Ringer, A. L.; Figgs, M. S.; Sinnokrot, M. O.; Sherrill, C. D. *J. Phys. Chem. A* **2006**, *110*, 10822−10828.